UNCERTAINTIES OF MULTI-DECADAL BUOY AND ALTIMETER OBSERVATIONS

A THESIS SUBMITTED TO THE GRADUATE DIVISION OF THE
UNIVERSITY OF HAWAIʻI AT MĀNOA IN PARTIAL FULFILLMENT
OF THE REQUIREMENTS FOR THE DEGREE OF

MASTER OF SCIENCE

IN

OCEAN AND RESOURCES ENGINEERING

AUGUST 2020

By

David J. Leyva

Thesis Committee:

Justin E. Stopa, Chairperson
Kwok F. Cheung
Philip R. Thompson
Clarence O. Collins

Dedication

This thesis is dedicated to my grandfather Fernando René Leyva
who believed it was important to never cease seeking the truth

Acknowledgments

This thesis was completed with the help and support of UH faculty as well as industry professionals. We would like to particularly acknowledge the advisor for this thesis, Dr. Stopa. We would also like to acknowledge the other committee members, Dr. Cheung, Dr. Thompson, and Dr. Collins. Also contributing support for this thesis were Robert Jensen of the U.S. Army Corps of Engineers along with Steven Dinapoli of Pacific Architects and Engineers. We would also like to acknowledge the organizations and data providers that were used for this thesis; Globwave, IFREMER, National Data Buoy Center, Marine Environmental Data Section, Coastal Data Information Program, OceanSITES, Integrated Marine Observing System, and Autralian Ocean Data Network.

Abstract

The impacts of climate change are evident globally. Changes to the sea state, including ocean wave heights, are important for the long-term design of oceanic infrastructure as well as resource extraction. Previous studies have estimated trends of wave height from multi-decade satellite altimetry and wave buoy observations but they do not robustly quantify uncertainties in trends. Changes to buoy hulls, payloads, and processors can introduce step changes and thus may influence year-to-year variability in the buoy time series which can create spurious climate signals. We find that standard approaches to identify step-changes in buoy time series are highly dependent on the reference time series. This is because identifying step-changes is most effective when analyzing a difference series, which is derived from the original time series minus a reference series. However, in the absence of a reliable reference series this method becomes subjective due to differences in reference series, (different hindcast products or different altimeter products). Therefore we adopt another approach which estimates uncertainties in multi-decadal wave height trends of buoy observations by extrapolating co-located altimeter-buoy wave height residuals. Synthetic wave height time series are created by randomly applying altimeter-buoy residuals to the original buoy time series through Monte Carlo simulations. The uncertainties of the buoy wave height trends are on the order of millimeters per year. This is relatively small when compared to the magnitudes of the buoy wave height trends which are on the order of centimeters per year and suggests that changes to buoy configurations are not having a large impact on the overall buoy trends. These synthetic time series provide a unique perspective into understanding wave climate and represent the uncertainty of buoy time series based on the differences between buoy and altimeters.

Table of Contents

List of Tables

List of Figures

Chapter 1

Introduction

1.1 Background

Global warming is causing many observable changes to Earth's climate. The warming of the planet includes a significant warming of the oceans which has the potential to drive considerable changes globally (Roemmich et al. 2015). Warmer ocean surface temperatures are being linked to an increase in the frequency of extreme El Niño events (Cai et al. 2014). Increases in precipitation rates have been recorded globally (Wentz et al. 2007). Along with this, large waves coupled with high tides and sea level rise have caused coastal inundation events across the western Pacific (Hoeke et al. 2013) and across the north Atlantic into the Caribbean (Lefèvre 2009). The warming being seen across the planet is unprecedented and although there have been time periods identified as "cold and warm epochs," there is no evidence to suggest that these epochs were consistently warm or consistently cold across the entire globe during the same time period, as is being observed now (Neukom et al. 2019). A large portion of this global warming has been linked to anthropogenic activity through release of carbon into the atmosphere (Koch et al. 2019).

Among the changes to climate occurring, one of particular importance is the variability in wind-generated surface gravity waves (called waves hereafter). Some studies report that wave heights are increasing as a result of increases in global winds, observed through satellite altimetry (Young et al. 2011). Separate studies using global reanalysis models have also estimated trends in global winds and waves (Fan et al. 2014; Aarnes et al. 2015). Reanalysis

winds are used to force wave hindcasts which are validated with buoy and altimeter datasets (Chawla et al. 2013; Stopa et al. 2019).

For an ocean engineer, understanding these changes is critical because environmental conditions such as wave height and sea level are used to define the criteria for coastal and offshore design. Many coastal and offshore structures are built to withstand extreme wave conditions projected from 50 to 1000 -year storms, with these extreme wave conditions being estimated from large wave events recorded in the historical period. However, if wave heights are increasing (or decreasing) projections for these storms would need to have this rate of increase (or decrease) included in the calculation methods. Studies using satellite altimetry data estimate extreme wave events and correlate them to climate indices, which is important for long-term planning (Izaguirre et al. 2011). Another method to assess the likelihood of extreme wave events in a particular location is to use long-term data sets with sufficient spatial resolution compiled through reanalyses databases (Reguero et al. 2012). Understanding the variability of wave heights at a regional level is important as well because even if there is a global trend of increasing wave heights studies have also identified specific locations where wave heights are expected to decrease (e.g., Shimura et al. 2016).

There are many different datasets used to study wave climate. Buoys measure the wave conditions in situ and have high temporal resolution (Menéndez et al. 2009). Satellite altimetry estimates significant wave height with expansive global coverage; however, these observations are not in situ and they rely on buoy measurements for calibration (Young et al. 2017). Humans aboard voluntary observing ships (VOS) report significant wave heights and these data are consistent with other data sources (e.g., altimetry, wave hindcasts) (Gulev and Grigorieva 2006). Wave hincasts are another source of wave information, and while they are not observations they have the advantage of having very high temporal and spatial resolution (e.g., Stopa 2018).

Recent works studying multi-decadal trends of significant wave height from 1985 to 2018 using satellite altimetry data report that there are a similar amount of increasing versus decreasing trends in mean significant wave heights globally, while there are primarily increasing trends in 90th percentile significant wave heights (Young and Ribal 2019). This is important because engineering design conditions are often based on extreme waves. If wave heights are increasing significantly at the higher percentiles this has the potential to put many coastal and offshore structures at risk, among other concerns.

Despite the over 40 year time series of many buoys, there are only a few studies which report climate change from these data records, most of which focus on the northeast Pacific (Allan and Komar 2000), (Gower 2002), (Menéndez et al. 2008), (Ruggiero et al. 2010). However, these studies do not account for changes to buoy configurations which can create spurious biases within the time series (Gemmrich et al. 2011). Trends of wave heights reported from previous studies for buoys WMO46005 (deployed off of the Washington coast) and WMO46002 (deployed off of the Oregon coast) along with projected 50 year increases are summarized in Table 1.1.

The first four studies are impacted by a bias in the early buoy data records caused by a constraint on the individual wave height limits in early processing techniques (Gemmrich et al. 2011). The low bias of those early buoy observations skew trend estimates to be positive. Gemmrich et al. (2011) analyzed buoy data records for inconsistencies, corrected the data records for these inconsistencies, and then estimated trends. The trends computed in Gemmrich et al. (2011), are much smaller in magnitude relative to the other studies ranging from -0.008 to 0.009 myr^{-1}.

Table 1.1 Buoy WMO46005 is deployed off of the coast of the state of Washington and buoy WMO46002 is deployed off of the coast of the state of Oregon, both along the USA west coast. Trends are estimated for annual averages and 50 year increases in wave height are calculated from these trends (assuming a continuous linear rate).

46005 Trend	*46005 50-yr*	*46002 Trend*	*46002 50-yr*	*Study*
2.7 $cmyr^{-1}$	135 cm	1.3 $cmyr^{-1}$	65 cm	(Allan and Komar 2000)
2.1 $cmyr^{-1}$	105 cm	1.9 $cmyr^{-1}$	95 cm	(Gower 2002)
2.0 $cmyr^{-1}$	100 cm	2.0 $cmyr^{-1}$	100 cm	(Menéndez et al. 2009)
1.5 $cmyr^{-1}$	75 cm	1.0 $cmyr^{-1}$	50 cm	(Ruggiero et al. 2010)
0.3 $cmyr^{-1}$	15 cm	-0.2 $cmyr^{-1}$	-10 cm	(Gemmrich et al. 2011)

1.2 Multi-Decadal Trends from Observations

To date, there are only a few studies that estimate multi-decade trends from observations, namely those from satellite altimetry (Young et al. 2011; Young and Ribal 2019). Young et al. (2011) and Young and Ribal (2019) estimate uncertainty using the seasonal Mann-Kendall test which estimates uncertainty from the altimetry dataset in a qualitative manner and reports the trend as significant or not. The other works using buoy observations have minimal emphasis on estimating uncertainty directly from the buoy datasets. A recent study by Timmermans et al. (2020) analyzes altimeter and hindcast data from 1992-2017 and reports January-February-March mean trends globally within the range of -0.04 myr^{-1} to 0.04 myr^{-1}. They suggest that certain regions of the globe have inconsistent trends. Therefore, in this work we focus our efforts on estimating trends from observational data records over the past several decades.

Recent efforts from several institutions and organizations worldwide have quality assessed and controlled buoy datasets and made them openly available. For example, the National

Data Buoy Center (NDBC) has collected wave information from buoys since the 1970's in the oceanic and coastal waters near the United States of America (USA). These datasets now extend several decades and cover many regions worldwide. These data could potentially be used to estimate multi-decadal trends to complement the work from satellite altimetry, VOS, and reanalysis-driven hindcasts. Therefore, our conjecture is that the multi-decadal buoy observations will point to new insights of the wave climate. However, caution must be exercised since Gemmrich et al. (2011) reports that changes to buoy hulls, payloads, and processors result in spurious trends. In this work we address the following scientific questions:

1) Can we identify non-climatic changes in buoy wave height records, and if so which changes to buoy configurations have a significant impact on the associated buoy trends?

2) What is the amount of uncertainty induced on buoy trends due to changes to buoy configurations?

3) Are there significant differences between mean trends and higher percentile trends (i.e., 90th and 99th percentile)?

1.3 Approach

To address the questions posed in the previous section we will first identify a diverse selection of buoys covering important regions of the global ocean. Next we adapt the approach of Gemmrich et al. (2011) and use the RHtestsV4 software (Wang and Feng 2013) to identify inhomogeneities in significant wave height data records from buoys. RHtestsV4 is a robust software for identifying changes in time series data and has been applied to air temperature

(Wang et al. 2007), air pressure (Wang 2008), rainfall rates (Wang and Feng 2009), and wind speeds (Wan et al. 2010) time series. There are less examples of using the software for analyzing significant wave height time series (Gemmrich et al. 2011; Aarnes et al. 2015; Thomas and Swail 2009). When searching for spurious changes in data records using RHtestsV4, it is recommended that a reliable reference dataset is used because the residual time series often highlight discrepancies better (Wang and Feng 2013). In this work, we utilize a number of different reference time series from satellite altimetry (Ribal and Young, 2020; Dodet et al., 2020) and an ensemble of wave hindcasts (Stopa 2018; Stopa et al. 2019). Specifically to address question one, we use RHtestsV4 to identify potential times or "change points" where the data quality of significant wave heights from buoy observations changes. In order to assess the change points, metadata is essential. To cross-reference our results from RHtestsV4, we use an alternate method to independently identify change points through a technique called "zonation." We are then able to assess the validity of the previous studies methodologies to identify change points and the resulting impacts on computed multi-decadal trends.

With neither of the methods to identify change points within the buoy time series yielding consistent results a new approach is developed. The goal of the new method we develop is not to identify change points within the buoy time series. We specifically address question two and quantify the uncertainty associated with the buoy time series. We calculate the differences between co-located altimeter-buoy data in order to understand the distribution and magnitude of buoy "errors." However, inherent in these residuals are also the errors from the altimetry data set. This results in residuals that are some times greater than the actual buoy error from the true value of significant wave height and it also results in residuals that are some times smaller than the actual buoy error. We randomly propagate these residual values onto the original significant wave height values from the original buoy time series. This creates a synthetic time series which varies from the original buoy time series relative to the

altimeter-buoy residuals. Creating many iterations of these synthetic time series establishes an uncertainty range for the buoy time series, and the range of the trends estimated from the synthetic time series establishes an uncertainty range for the buoy trends. These uncertainty ranges quantify the impact of changes to buoy configurations on the associated buoy trends.

Finally, to address question three we calculate yearly statistics from the synthetic time series. Specifically, we compare uncertainties of annual mean, annual 90th percentile, and annual 99th percentile trends. We also compare the magnitudes of estimated trends from the synthetic time series to trends from previous studies using satellite altimetry (Young and Ribal 2019).

1.4 Thesis Outline

The thesis is outlined as follows. In chapter two, we describe the various data sets used in this study. We detail our buoy selection criteria and auxiliary reference datasets including satellite altimetry and wave hindcasts. Next, in chapter three, we describe our approach of identifying change points in significant wave height time series through RHtestsV4 and zonation and present our results for specific buoys. In chapter four, we first describe our method to create synthetic time series using residuals from co-located altimeter-buoy significant wave height observations. We then estimate trends from these synthetic time series along with the associated uncertainties. In chapter five, we discuss the implications of our findings relative to questions one, two, and three. We highlight regional trends based on our results from chapter four. We also discuss how buoys will be used in the future and the importance of keeping metadata records of buoy configuration. Lastly, we summarize our overall findings and provide recommendations for future research.

Chapter 2

Datasets

2.1 Buoys

2.1.1 Background

Buoys are a proven way to collect in-situ sea state data (Menéndez et al. 2009; Longuet-Higgins 1984). Typically buoys are moored to the seafloor to prevent the buoy from drifting. The buoy platforms support many different instruments which measure different oceanic and atmospheric quantities (Steele et al. 1998). Wave information including 1-dimensional (1-D) (frequency vs. energy) and 2-D (frequency-direction vs. energy) spectra are essential information that describe the sea state (Ardhuin et al. 2019). Buoy hull motion is measured by accelerometers which are typically located within the hull of the buoy. Buoys that only report wave frequency-spectra (1-D) use a single accelerometer to measure acceleration along the vertical axis of the buoy (heave motion). Many buoys that report the wave energy distribution as a function of wave frequency and direction (2-D) measure additional properties of the sea surface (Steele et al. 1998). Buoy hull vertical displacement (elevation) can be derived from a single accelerometer by taking a double integration of the heave acceleration. Detailed descriptions of how frequency-direction spectra are calculated can be found in prior works (Longuet-Higgins 1957; Longuet-Higgins 1980; Steele and Earle 1991).

To calculate significant wave height a Fast Fourier Transform (FFT) (Brigham 1988) is applied to the buoy heave motion data which converts it into the frequency domain to give

the heave spectrum. This is done in order to represent the buoy elevation as a summation of regular waves. Using the spectral method the time series is decomposed into many waves with different harmonics (frequencies). Response amplitude operator (RAO) processing needs to be done on the data in the frequency domain because the hull of the buoy as well as electronic noise need to be accounted for in the calculations (N. NDBC 2018). The RAO processing relates the motion of the buoy to the motion of the sea surface. From the RAO, the sea surface elevation (h) can be calculated (N. NDBC 2018). Significant wave height, defined as the average wave height of the highest one third of the waves, can be represented by equation 2.1 where $E(f)$ is the heave spectrum.

$$H_s = 4\sqrt{\int_0^\infty E(f)df} \tag{2.1}$$

It has been shown that the quality of significant wave height measurements can be affected by changes to buoy configuration (Gemmrich et al. 2011). Documented changes to buoy configuration include changes to hull size/type (N. NDBC 2012), payload (on-board computer system) (N. NDBC 2017), and data processor (N. NDBC 2018). In the following section, these components are briefly summarized.

2.1.2 Open Source Datasets

The buoy data considered for this study are from the following networks; National Data Buoy Center (NDBC), Marine Environmental Data Section (MEDS), Coastal Data Information Program (CDIP), OceanSITES, and Integrated Marine Observing System (IMOS). Incorporating each of these networks allows for a wider spatial expanse of the observations because each network has a regional focus. *L'Institut Français pour la Recherche et l'Exploitation de la Mer* (IFREMER) has cataloged buoy data from NDBC, MEDS, CDIP, and OceanSITES through the GlobWAVE project (globwave.ifremer.fr/). GlobWAVE focuses on producing

observational sea state information mainly from satellite observations. This project is now extended through a European Space Agency (ESA) project called the Sea State Climate Change Initiative (CCI). The IMOS buoy data is available directly from the Australian Ocean Data Network (AODN). The available buoys along with their length of deployment are shown in Fig. 2.1 across the five networks.

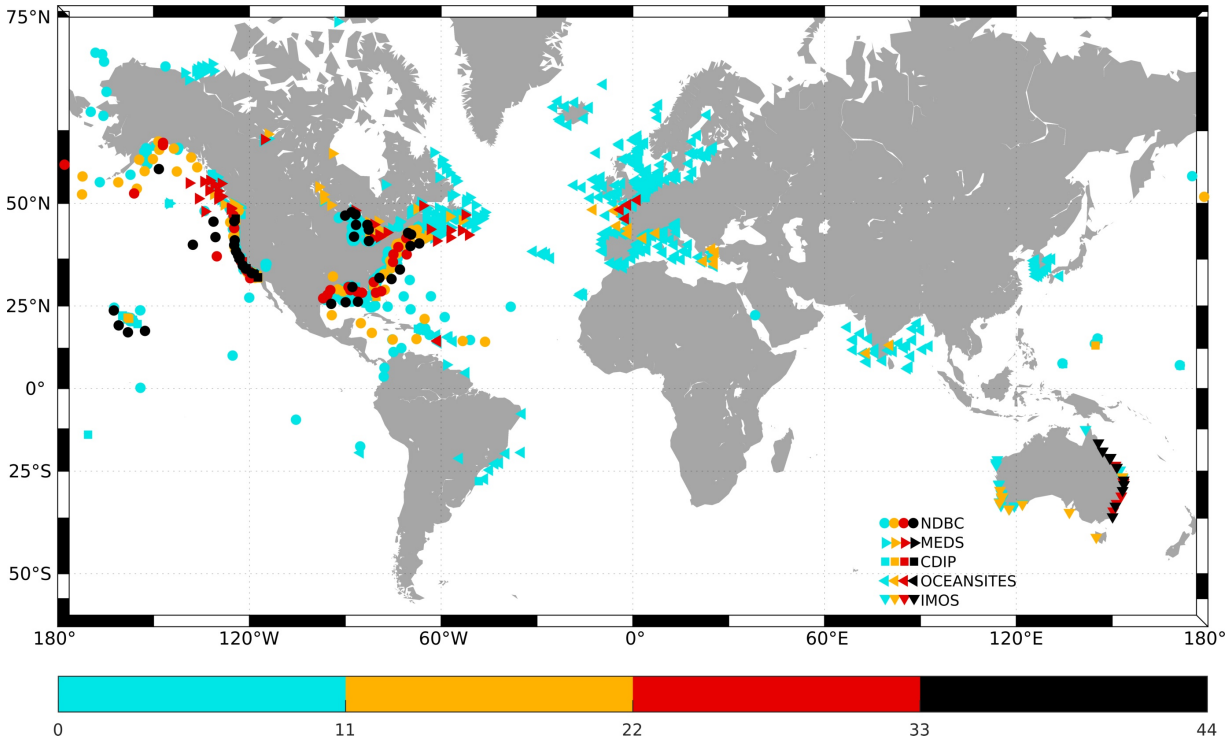

Figure 2.1 Buoy locations for NDBC, MEDS, CDIP, OceanSITES, and IMOS. The color represents the length of deployment and the symbol represents the network.

The goal of NDBC is to provide real-time observations in the marine environment. They strive to ensure that the observations are of high quality while being obtained in a safe and sustainable manner. The data is made open source so that it can be used to improve predictions of weather. They have operated and maintained buoys in oceanic and coastal waters near US coastlines since the 1970's. From the NDBC network, 370 buoys were considered. Many of these buoys have data records exceeding 40 years. There are buoys deployed along

the US east and west coasts, along the Alaskan coast, within the Gulf of Mexico, throughout the Caribbean, and around Hawai'i. Additionally, there are buoys deployed near South America, the equatorial Pacific, the Bering Sea, Guam, and within the Arctic. The NDBC network covers expansive regions of the global ocean. NDBC has used different buoy hulls, payloads, and processors which are documented in metadata for many of the buoys and can be found online at (https://www.ndbc.noaa.gov/data_availability/data_avail.php).

MEDS is operated by the government of Canada. The goal of MEDS is to provide observations to be used for weather forecasts around Canada. From the MEDS network 356 buoys were considered. The majority of these buoys are deployed along the Canadian east and west coasts. There are also several buoys located in the Arctic Ocean. Choosing buoys from this network helps to fill in any regional gaps that were not covered by the NDBC network. MEDS has also made changes to buoy configurations over the years and many of the buoy hulls used by MEDS are the same types of hulls used by NDBC. There is only a limited amount of metadata available for MEDS buoys which can be found online at (http://www.meds-sdmm.dfo-mpo.gc.ca/isdm-gdsi/waves-vagues/index-eng.htm).

The goal of CDIP is to improve the nearshore wave climatology for the United States in order to better inform coastal planners and engineers. Along with this, they provide real-time data that is used in both professional as well as recreational settings by a variety of users. From the CDIP network 232 buoys were considered. The majority of these buoys are deployed along the US East and West coasts, and along the Alaskan coast. Only a few of these buoys have deployments greater than 20 years, all of which are located along the US west coast. CDIP moored buoys are Datawell Waveriders and detailed information about these buoys is available online at (https://www.datawell.nl/products/buoys.aspx). The buoys have comprehensive metadata records which can be found on the CDIP website at (https://cdip.ucsd.edu/).

Table 2.1 The total number of buoys in the NDBC, MEDS, CDIP, OceanSITES, and IMOS networks, grouped by range of years deployed.

Years Deployed	0 - 11	12 - 22	23 - 33	34 - 44
NDBC	247	59	27	37
MEDS	304	24	28	0
CDIP	195	28	2	7
OceanSITES	403	14	6	0
IMOS	27	9	6	10

The goal of OceanSITES is to collect and deliver high quality ocean data. OceanSITES strives to collect multinational data, particularly around the European coast where the diverse coastline leads to multiple entities collecting data in a relatively small region. The incorporation of data from these entities into one network helps to facilitate the use and analysis of data throughout the region. From the OceanSITES network 423 buoys were considered. However, the majority of these buoys have deployments of less than 5 years. The buoys are primarily deployed around Europe, with some around South America, the Caribbean, Africa, India, and Korea.

The goal of IMOS is to collect multi-institutional ocean data within Australia and make it openly available. This data is made available to the marine and climate science community. The Australian Ocean Data Network (AODN) merged with IMOS in 2016 which has a focus on open data access. From the IMOS network 52 buoys were considered. The buoys along the Australian west and south coasts have deployments less than 20 years. Along the Australian east coast many of the buoys have deployments greater than 40 years. IMOS moored buoys are Datawell Waveriders which report 1-D as well as 2-D wave spectra. There is limited metadata available for the buoys online at (https://portal.aodn.org.au/).

The number of buoys available for each network is shown in Table 2.1. The buoys are further grouped by their lengths of deployment, defined as the number of years from the initial to the final deployment.

Throughout the years, changes to buoy designs have included hull shape and size. The major types of NDBC buoy hulls are shown in Fig. 2.2.

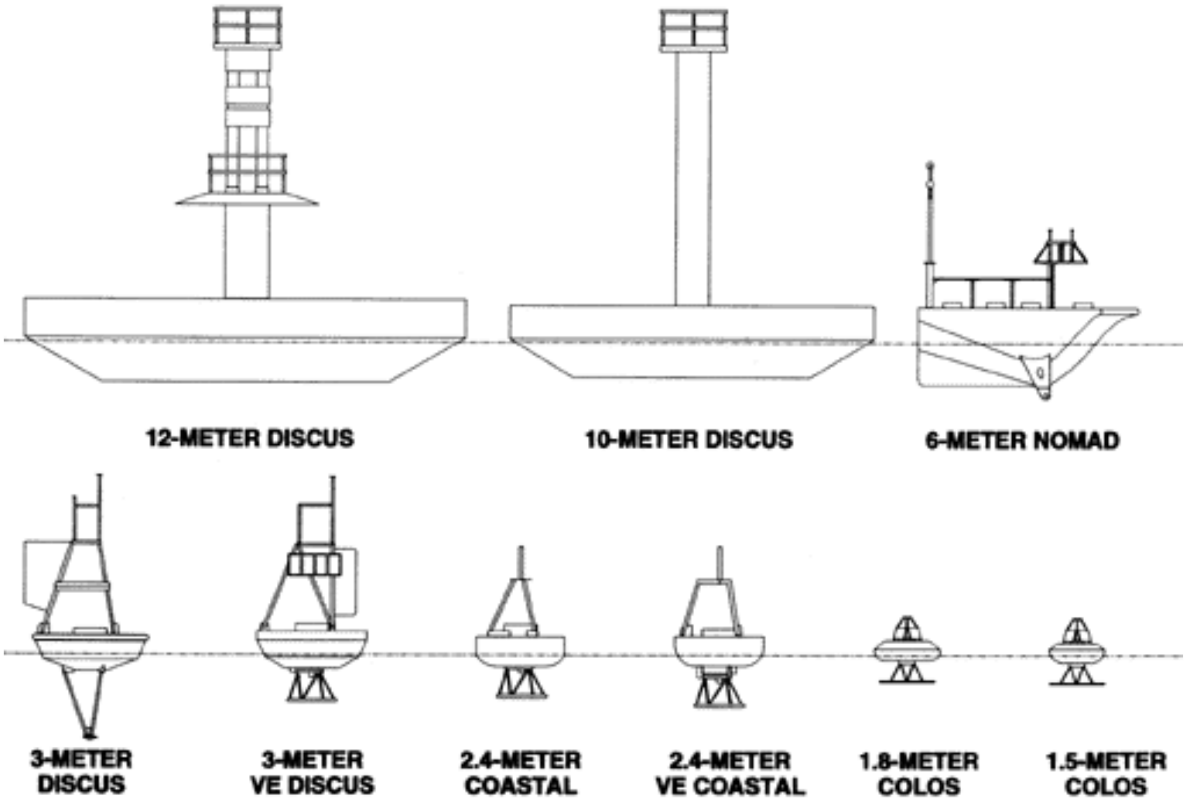

Figure 2.2 Examples of some of the most common hull types used by NDBC (NOAA 2014)

.

The primary buoy types that have been used are the 12-meter discus, the 10-meter discus, the 6-meter Navy Oceanographic Meteorological Automatic Device (NOMAD), and the 3-meter discus. The discus buoys have similar shapes, with different diameters. However, some discus buoys have been known to capsize (N. NDBC 2018), but the NOMAD buoy

has not had a recorded instance of capsizing with the boat like hull increasing stability. For this reason the NOMAD buoy has been deployed in locations that are exposed to harsh conditions.

Other networks use some of the same types of buoys as NDBC as well as other types of buoys. The MEDS network has commonly used the 6-meter NOMAD buoy for deployments. The CDIP and IMOS networks both use the Datawell Waverider buoys shown in Fig. 2.3. These buoys have a spherical hull of either 0.9 meters or 0.7 meters (Datawell 2020). Appendix E contains images of buoys collected from different references.

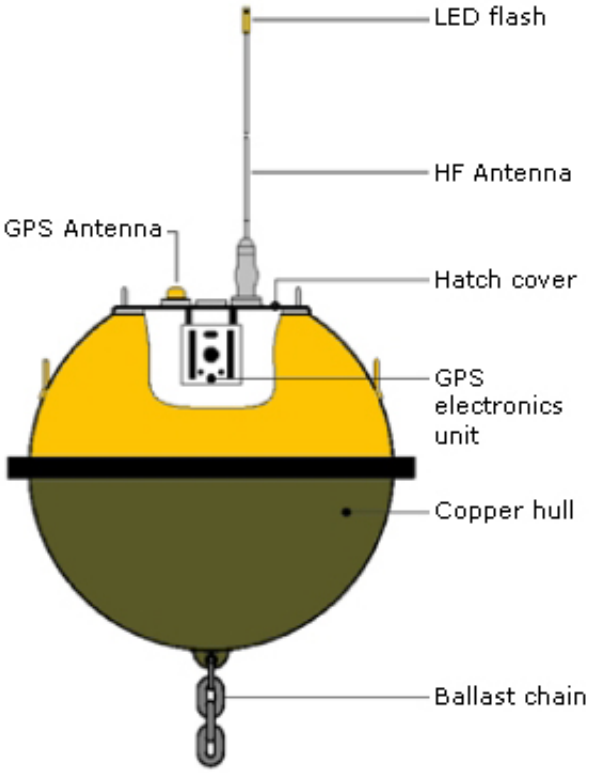

Figure 2.3 Datawell Waverider Buoy (Queensland Government 2019)

Another buoy component that has changed over the years is the payload. This is the on-board computer system used in the collection of the heave data and in the calculation of

Table 2.2 NDBC Payloads

Abbreviation	Payload Name
ARES	Acquisition and Reporting Environmental System
DACS	Data Acquisition and Control System
DACT	Data Acquisition and Control Telemetry
EEP	Engineering Evaluation Phase
GSBP	General Service Buoy Payload
MARS	Multifunction Acquisition and Reporting System
PEB	Prototype Environmental Buoy
SCOOP	Self-Contained Ocean Observations Payload
UDACS	UHF Data Acquisition and Control System
UDACS(A)	UDACS with WDA processor instead of WSA
VEEP	Value Engineered Environmental Payload

Table 2.3 NDBC Processors

Abbreviation	Processor Name
EEP	Engineering Evaluation Phase
WSA	Wave System Analyzer
WDA	Wave Data Analyzer
WA	Wave Analyzer
WPM	Wave Processing Module
DWPM	Directional Waves Processing Module
DDWM	Digital Directional Wave Module

significant wave height. For NDBC payloads the most common specified tolerance on wave height is ±0.2 m (N. NDBC 2017). The NDBC network has implemented many different payloads throughout the years and a summary is given in Table 2.2.

One part of the payload system is the processor which is the specific software and technique used to process the data (N. NDBC 2009). Also noted in (Gemmrich et al. 2011) was that different processors have been used over the years with different configurations involving corrections for low frequency noise, the numbers of spectral bands, low frequency resolution, among other important characteristics. A summary of different processors used by the NDBC network is given in Table 2.3

2.1.3 Metadata

There are many different types of metadata associated with buoys. The metadata compiled in (Gemmrich et al. 2011) are the hull, payload, and processor. Other metadata include but are not limited to; latitude and longitude of the buoy, depth of the buoy, mooring configuration, buoy service dates, and buoy deployment dates. Each individual buoy also has a unique serial number which can be used to track specific buoys and the locations where they are deployed. Buoy serial numbers are important because each buoy model has certain specifications. Acceptable variations between buoys of the same model type will likely result in buoys of the same model type reporting different values for significant wave height. The difference between service dates and deployment dates is that a buoy could be serviced in some way (such as cleaning due to bio-fouling) and after the servicing the buoy remains deployed as it was before servicing. Buoy deployment dates specify when a unique buoy hull identification number is deployed in one location with one configuration. For example, if one 10-meter discus buoy is changed with another 10-meter discus buoy, this is regarded as two separate deployments for the purposes of the metadata in this study. Buoy deployment

dates can be identified if the unique serial number for each buoy is recorded in the metadata.

Each network has a unique method to report metadata. On the NDBC website there are metadata, (https://www.ndbc.noaa.gov/data_availability/data_avail.php), available until 2003. After 2003, metadata exist however they have not been compiled and made available to the public. Robert Jensen of the US Army Corps of Engineers (USACE) and Steven Dinapoli of NDBC Pacific Architects and Engineers (PAE) have compiled metadata which is more comprehensive than the metadata available on the NDBC website. On the MEDS website (http://www.meds-sdmm.dfo-mpo.gc.ca/isdm-gdsi/waves-vagues/index-eng.htm) there are metadata records available. However, these records only exist from 1997 to 2014. On the CDIP website (https://cdip.ucsd.edu/) there are comprehensive metadata records for each buoy. For OceanSITES metadata is not easily accessible. There is likely metadata available for some of the OceanSITES buoys, but it is not clear where this is contained and as a result no metadata for OceanSITES buoys are used for this study. For the IMOS buoys there is limited metadata available within the netcdf files which can be downloaded from the AODN website (https://portal.aodn.org.au/). However, the IMOS buoys fall within four different governing bodies within Australia each with their own unique practices in regards to compiling and storing metadata. By contacting members from the four different governing bodies within Australia it is possible to access additional metadata records.

The different types of metadata compiled for this study are; hull, payload, latitude and longitude, buoy service dates and buoy deployment dates. From NDBC and MEDS the metadata compiled for this study are; hull, payload, latitude and longitude, and buoy service dates. From CDIP the metadata compiled are the same as the metadata compiled for NDBC and MEDS with the addition of metadata indicating buoy deployment dates. From IMOS the only metadata compiled are; hull and buoy deployment.

CDIP and IMOS buoys are Datawell Waveriders. The CDIP buoys selected for this study

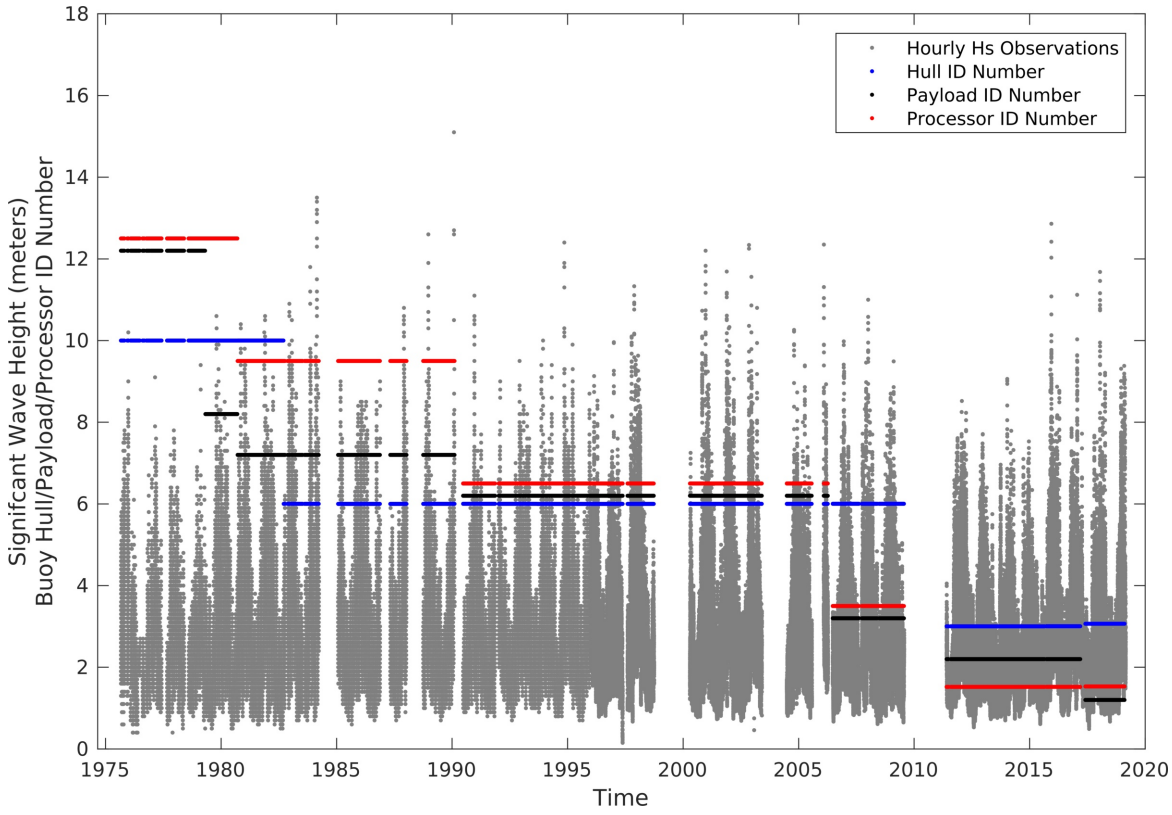

Figure 2.4 Hourly significant wave height observations over 44 years for NDBC buoy WMO46002 with hull, payload, and processor changes indicated by blue, black, and red horizontal lines. The metadata is linked to the y-axis and for hulls it represents the buoy diameter (or buoy length) in meters. For payloads and processors the older models are indicated by larger numbers on the y-axis and newer models are indicated by smaller numbers.

were all confirmed to be directional (the wave data includes information on the direction the waves are propagating from). Of the IMOS buoys, some are directional while others are non-directional.

An hourly time series of significant wave height observations is shown in Fig. 2.4 for buoy WMO46002 with changes to the hull, payload, and processor indicated. It should be noted that the types of processors that limited individual wave height measurements to ± 11 m correspond to numbers of ten and above on the y-axis. With the metadata presented in

this way it can clearly be seen that when the processor is above ten on the y-axis values for significant wave height rarely exceed 10 m, and when this processor changes to a value below ten there is an increase in values of observed significant wave height. The other compiled metadata can be overlaid as well and also have the potential of providing useful insights. The hull, payload, and processor id numbering system is described in detail in Appendix B.

2.1.4 Buoy Selection

Of the 1433 available buoys we selected a total of 50 buoys to be reviewed further for agreement with altimetry data. The locations and lengths of deployment of the selected buoys are shown in Fig. 2.5 for each of the five networks.

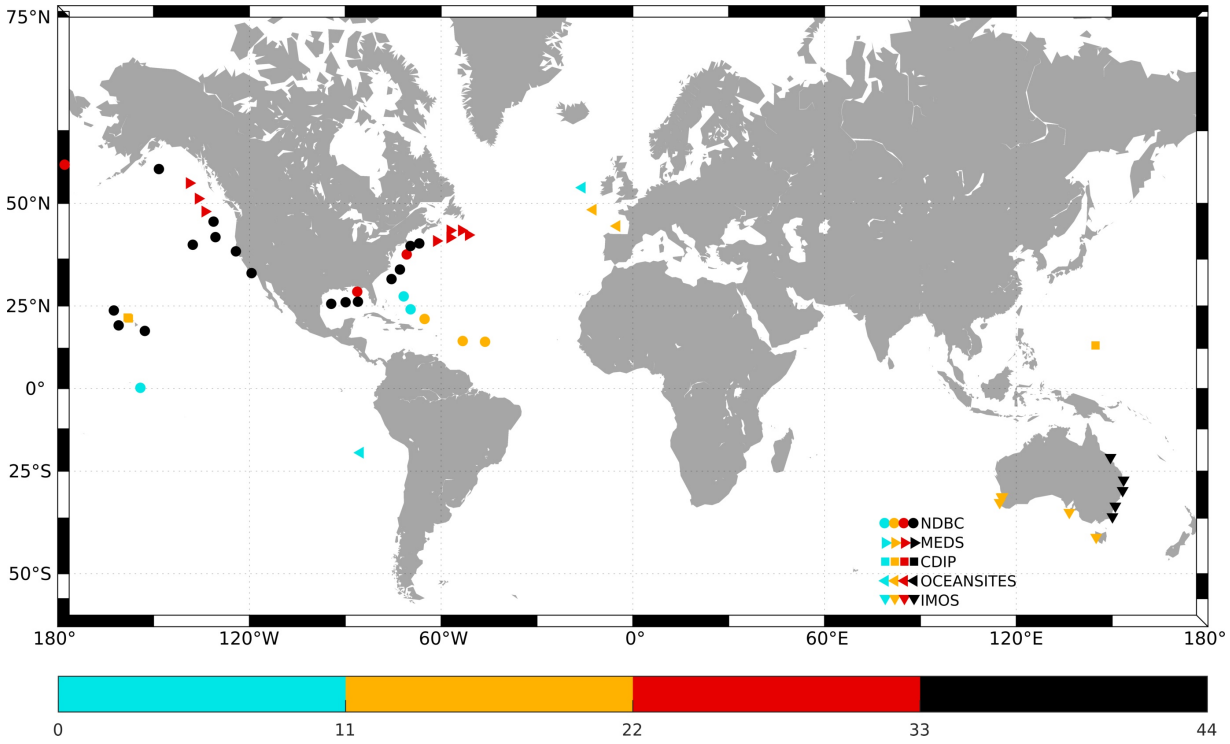

Figure 2.5 Buoys selected from the NDBC, MEDS, CDIP, OceanSITES, and IMOS networks, grouped by range of years deployed.

When selecting buoys for this study, there are many different criteria that are important.

A primary criterion is that the buoy has a long time series. The data records of available buoys go back as far as 1972, allowing for many time series to be greater than 40 years in length. There are also many buoys that have time series greater than 30 years in length. Buoys with this many years of data were considered most appropriate for this study in order to best identify long term trends in wave climate.

However, buoys with less than 30 years of data are considered as well, and are chosen if they met other important criteria. Buoys located in geographic regions with few or no other buoys are considered even if the time of deployment was short. In order to have adequate spatial coverage on a global scale some of the buoys that are chosen have time series just over 10 years in length. This trade-off of length of data record is deemed acceptable in order to improve global coverage.

Another important criterion of the selection process is that the buoys be deployed in relatively deep water. The reason for this is because deep water buoys will not be affected by shallow water dynamics such as refraction. Also, re-deploying a buoy in a slightly different location will not have an impact on wave heights due to the relatively minimal change in water depth. This criterion for selecting buoys in deep water is also an attractive requirement for co-locating buoy data with altimetry data. A further criterion for buoy selection is to avoid choosing buoys in the shadows of islands as these could be very sensitive to directional changes in swell which would impact the data. Similar criteria to these have been used in previous studies (Zieger et al. 2009).

A final criterion is that buoys should also be adequately distance from coastal features so that corresponding altimeter observations can be obtained for the location. An altimeter image footprint for older altimeters has a diameter of between five to ten kilometers (Young et al. 2017) and if any of this footprint covers land the entire image cannot be used, (note that for newer altimeters equipped with delayed Dopplers this is not the case). Regardless, this

criterion of distance from coastal features needs to be observed so that data from the entire altimetry record can be utilized rather than being limited to data from newer altimeters. Along with this, it can be computationally intensive for hindcasts to resolve coastal features precisely, so this would also make it difficult to compare coastal buoys with hindcast datasets.

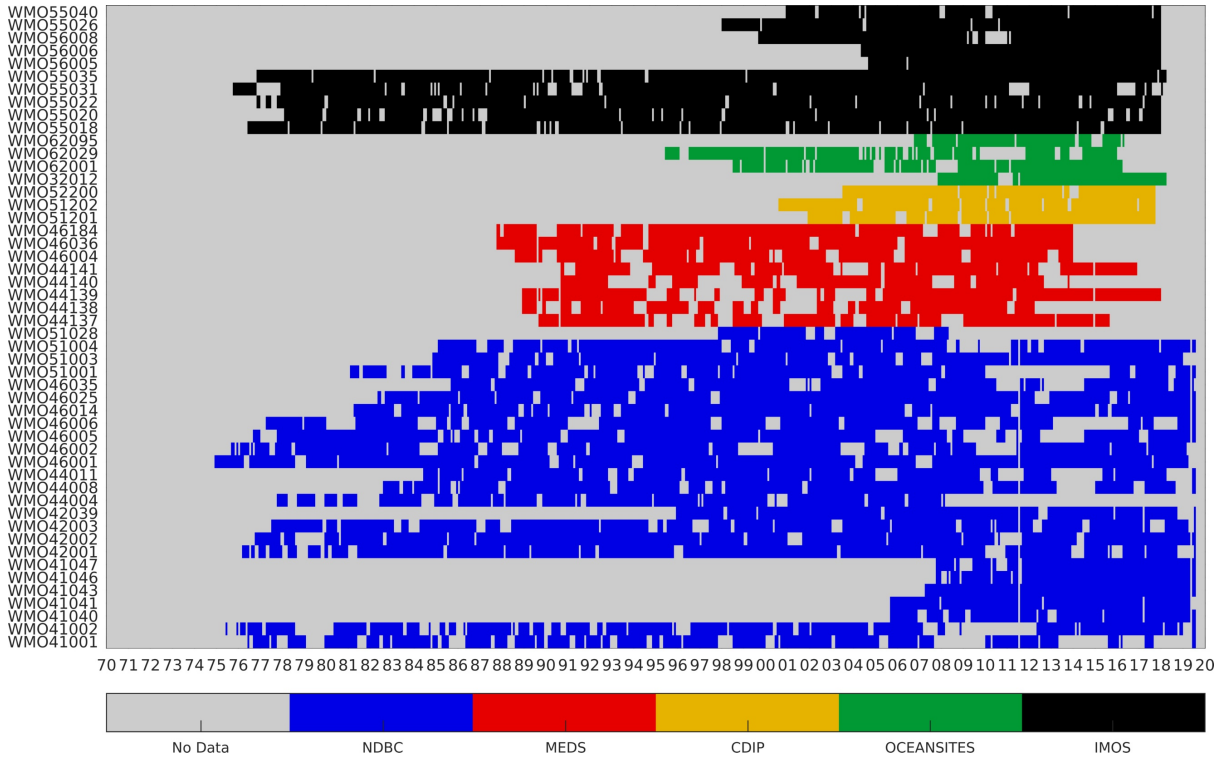

Figure 2.6 Buoy data gaps identified for each buoy and grouped by network. The color grey indicates no data and the colors associated with each network indicate data.

From the available buoys we select 25 buoys are from NDBC, 8 are from MEDS, 3 are from CDIP, 4 are from OceanSITES, and 10 are from IMOS. While length of deployment is important, it is also important that the time series have minimal data gaps. Data gaps can occur when the buoy is being serviced, when a sensor malfunctions, when a payload has errors in calculations, among other reasons. For the selected buoys Fig. 2.6 displays where there are gaps in the data records. The different colors indicate the network each buoy is

associated with and that there is data available during that time period, with grey indicating that no data is available.

2.2 Reference Datasets

2.2.1 Altimetry

The altimetry data sets begin in 1985 with the GEOSAT (Geodetic/Geophysical Satellite) mission. With just one satellite taking measurements some areas of the ocean would only have recorded observations two to three times a month. Having more satellites in orbit helps increase the number of recorded observations. However, altimetry datasets are still relatively sparse often not exceeding 20 observations per month. Many events that occur on short time scales can easily be missed by altimeters. The significant wave height calculated from the altimetry data depends on how the raw data is calibrated and processed and what specific algorithms are applied during the data manipulation.

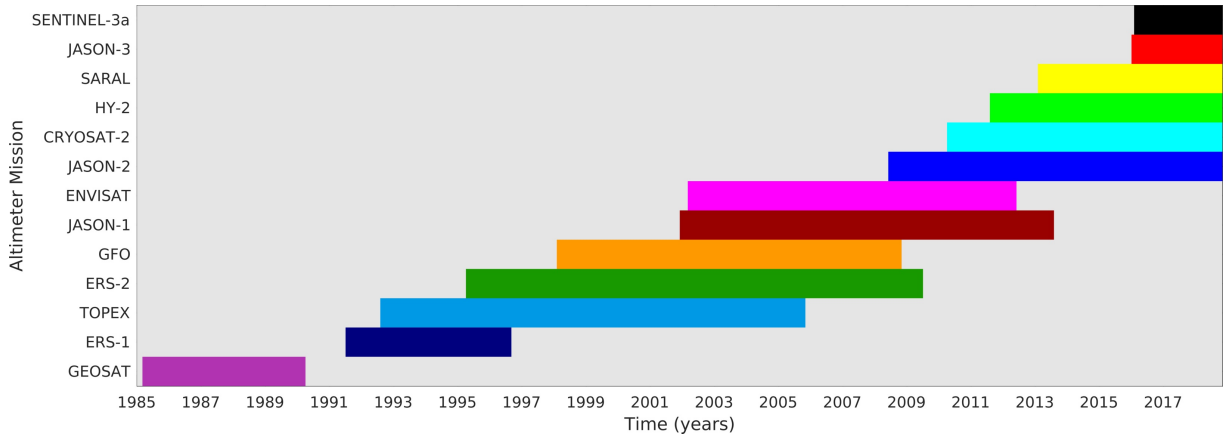

Figure 2.7 Years of deployment for different altimeter missions

The method used for the Ribal and Young dataset, referred to as "RY2019" hereafter, is described in their works (Ribal and Young 2019). IFREMER have their own distinct

methods for treating the raw data from altimeters. Altimetry data sets will be used in this study for comparison against buoy data. One reason that altimetry data is valuable for this study is because the time series can be assumed to be reasonably homogeneous. When multiple altimeters are in orbit there are times when two altimeters cross over one location of the ocean at the same time. These "cross-over points" are used to validate and cross-check the altimeters to make sure they are not drifting over time or giving spurious results (Young et al. 2017).

Validating altimetry data by co-locating multiple platforms helps to increase confidence in data homogeneity across altimeters. Having multiple altimeter missions deployed at the same time increases the amount of data gathered while also increasing the amount of co-locations in time and space for validation. The deployment years for the different altimeter missions from 1985 to 2020 are shown in Fig. 2.7.

Criteria that have been used to co-locate altimeter data with buoy data for calibration are that the altimeter track must have a minimum of five altimeter observations which occur within less than 50 km of the buoy location and within 30 minutes of the buoy observation (Young et al. 2017). We use the same criteria for this study to determine if the selected buoys are in locations which can be reasonably represented by altimeters.

By plotting the locations of the altimeter tracks it can be determined if there are any local coastal features which could impact the data as shown for buoy WMO46002 in Fig. 2.8 (a). Comparisons of the buoy and altimeter significant wave height observations are performed to verify that the co-located altimetry data are reasonable representations of the sea state observed by the buoy. Buoy WMO46002 shows good agreement with the co-located altimeter data with a correlation coefficient between buoy and altimeter observations of 0.99, a bias of 0.02 m, along with other statistics shown in Fig. 2.8(b).

For the comparison "N" represents the total number of co-located observations. "BIAS"

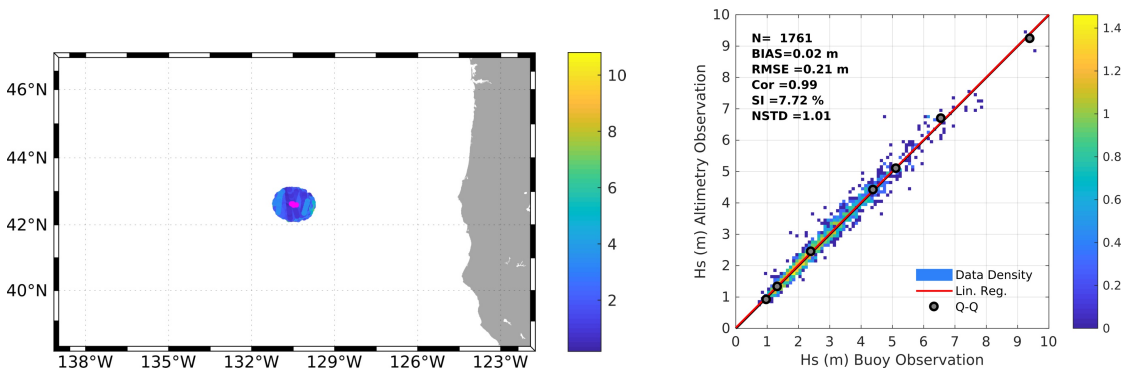

(a) Altimetry data co-located with buoy **(b)** H_s comparison

Figure 2.8 (left) RY2019 altimetry H_s data co-located within 50 km of the buoy WMO46002 (color indicates H_s in meters), and (right) comparison of buoy H_s observations versus altimetry H_s observations (color indicates log10 data density).

is the mean error, calculated by finding the sum of the differences between the two sets of observations and then dividing by the total number of observations. "RMSE" is the root mean square error, calculated by finding the differences between the two sets of observations, squaring the differences, finding the mean of these squared differences, and finally finding the square root of the mean of the squared differences. "Cor" is the correlation coefficient, calculated by finding the covariance of the two sets of observations normalized by the variance of each of the sets of observations. "NSTD" is the normalized standard deviation, which is calculated by finding the standard deviation of the altimetry set of observations and dividing by the standard deviation of the buoy set of observations.

Decreasing the window size for the altimetry data has the potential to improve agreement between buoy and altimetry observations. One reason for this is that in relatively shallow water with large depth gradients narrowing the window size for co-locating altimetry data generally results in the depth where the altimetry data is taken becoming more representative of the depth at the buoy location. However, decreasing the window size reduces the total number of possible altimeter-buoy co-locations, which is already subject to limited sampling. Also, in some situations even a very narrow window for altimeter data will not result in good

agreement between buoy data and altimeter data. The depth at buoy WMO56008, deployed off of the Australian west coast, is only 38 m. Even with a very small window size, the altimetry data is not a good representation of the buoy location as shown in Fig. 2.9.

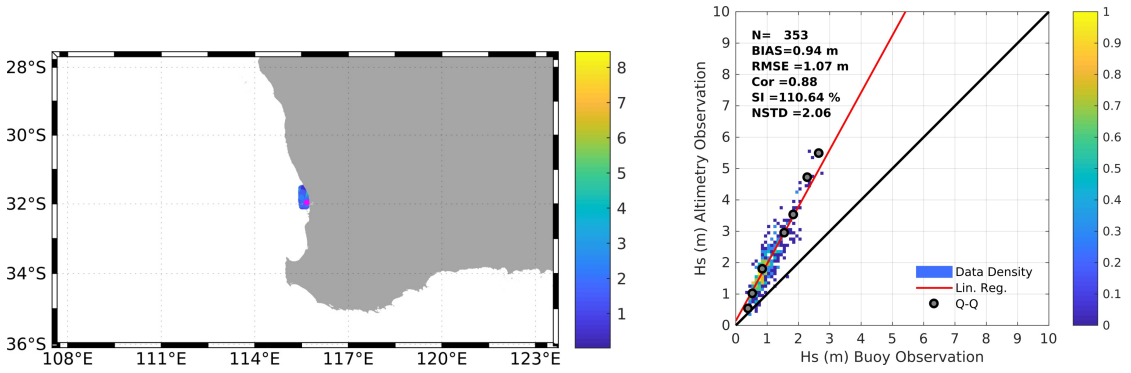

(a) Altimetry data co-located with buoy **(b)** H_s comparison

Figure 2.9 (left) RY2019 altimetry H_s data co-located within 50 km of the buoy WMO56008 (color indicates H_s in meters), and (right) comparison of buoy H_s observations versus altimeter H_s observations (color indicates log10 data density).

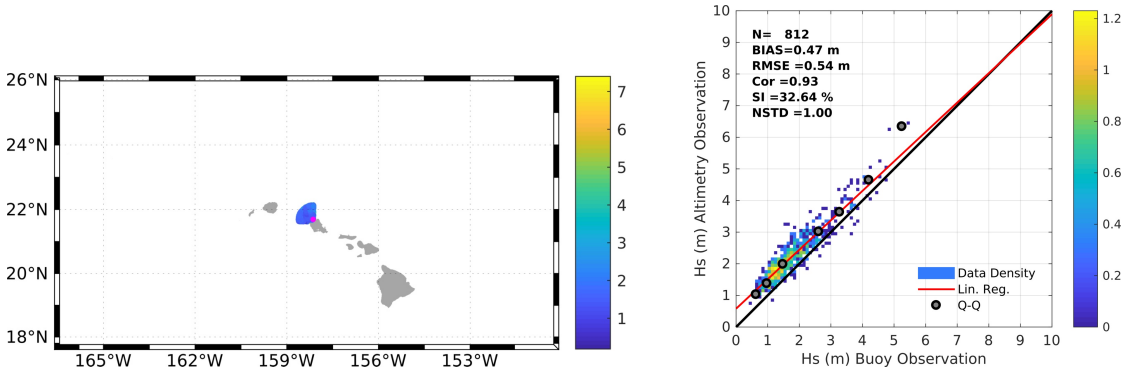

(a) Altimetry data co-located with buoy **(b)** H_s comparison

Figure 2.10 (left) RY2019 altimetry H_s data co-located within 50 km of the buoy WMO51201 (color indicates H_s in meters), and (right) comparison of buoy H_s observations versus altimeter H_s observations (color indicates log10 data density).

Also, if a buoy location is in the shadow of coastal features or islands the altimeter window needs to be carefully selected. An example of this is shown for buoy WMO51201 in Fig. 2.10, which is deployed off of Waimea Bay, O‘ahu, Hawai‘i. Altimetry data within 50

km of the buoy location is available on the north, and south sides of the island. However, data from the south side of the island will not be representative of the sea state at the buoy location on the north side of the island so this data is excluded.

Based on this analysis 4 of the 50 selected buoys are excluded from this study. The buoys that are excluded are as follows; buoy WMO56008 from the IMOS network, buoys WMO51202 and WMO5200 from the CDIP network, and buoy WMO46025 from the NDBC network. This leaves a total of 46 buoys to be included in this study.

2.2.2 Hindcasts

Hindcasts use wind reanalysis datasets to force an ocean model which outputs sea states globally. The forcing winds vary between hindcasts and this changes the output of significant wave height. The time resolution for hindcasts varies from one to six hours. The hindcasts we use for this study are CFSRMOD, ERA5, R20C, and SCT. Recent work shows that the differences in how hindcast products are created lead to significant differences in their estimations of significant wave height (Timmermans et al. 2020). The time periods that each hindcast has data for are shown in Table 2.4. Detailed information on each hindcast is recorded in (Stopa 2018) with a brief description of each provided below.

R20C is created by the National Center for Environmental Prediction (NCEP) and results are output every three hours (Compo et al. 2011). Air pressure is assimilated and observations go as far back as 1851. Data is assimilated using a Kalman Filter and sea ice is considered. The hindcast is available from 1979 to present.

CFSRMOD is similar to the CFSR hindcast with the modification of assimilating altimeter data to correct for hindcast biases. CFSR is created by NCEP and results are output every hour (Saha et al. 2014). Data is assimilated spatially in three dimensions and sea ice is considered. This is the only hindcast that uses a dynamic sea ice model. The hindcast is

Table 2.4 Time Periods of Hindcasts

Hindcast	Time Period
R20C	1979 - present
CFSRMOD	1979 - present
ERA5	1979 - present
SCT	1993 - present

available from 1979 to present.

ERA5 is created by (ECMWF), the European Center for Medium-Range Weather Forecasts. ERA5 replaces ERA-Interim which was stopped on August 31, 2019 and which has been used in previous studies (Aarnes et al. 2015). For ERA5 results are output every hour and the Earth is covered spatially in a 30 km grid. The first segment of the hindcast is available from 1979 to present and eventually the entire hindcast will be available from 1950 to present.

SCT is created by IFREMER and results are output every six hours (Bentamy et al. 2017). Data is assimilated using scatterometer data and sea ice is not considered. This composition of wind observations from satellites is available from 1993 to present.

Chapter 3

Data Homogeneity

3.1 Background

Inherent to all forms of data collection is the possibility that different data collection methods measuring the same quantity or phenomenon can produce different results due to random or systematic errors. For this reason, extensive calibration and validation needs to be performed before a data collection method can be qualified as acceptable. Acceptance criteria is based upon a specified tolerance range. Different applications will require different levels of precision which will make the tolerance ranges narrower or wider. In the case of buoys measuring wave height the tolerance ranges have generally been determined based on the precision needed for short-term weather and wave forecasts (Gemmrich et al. 2011). For most NDBC payloads, the tolerance on individual wave heights is ± 0.2 m (N. NDBC 2017). As buoy configurations change over the years, there is the possibility that different buoy configurations will result in different measurements of wave height within this specified level of tolerance.

3.1.1 RHtestsV4

One method that has been used to detect change points in data records is through the software package RHtestsV4 which uses various statistical analysis tests to detect inhomogeneities in time series (Wang and Feng 2013). Change points are locations within a data

series where an abrupt variation occurs in either the mean (step-type) or the slope (trend-type) of the data series (Wang 2003). Step changes and trend changes can be detected using a two-phase regression model as shown in equation 3.1 (Wang 2003), where ϵ_t represents zero-mean independent and random errors.

$$X_t = \begin{cases} \mu_1 + \alpha_1 t + \epsilon_t & 1 \leq t \leq c \\ \mu_2 + \alpha_2 t + \epsilon_t & c < t \leq n \end{cases} \tag{3.1}$$

For each time c that is evaluated, the determination of whether or not it is a change point is based on the difference between μ_1 and μ_2, and α_1 and α_2.

When using RHtestsV4 to analyze a time series (base series) it is recommended to also use a reliable reference. The difference between the base series and the reference series is analyzed, and in this difference series mean shifts are often more pronounced and statistical tests perform with increased certainty. When using a reference series RHtestsV4 implements a penalized maximal t-test (PMT) to determine if identified mean shifts are significant (Wang et al. 2007). The PMT test reduces the amount of change points detected when compared to the standard t-test which can result in the identification of erroneous change points, "false alarms." However, RHtestsV4 also has the option to analyze the time series in conjunction with metadata which documents instrumentation changes and in this analysis the standard t-test is used. In this case, only the change points identified that are supported by reliable metadata are identified as significant.

RHtestsV4 can also be implemented without a reference series. When analyzing the time series of interest (base series) without a reference series, RHtestsV4 uses a penalized maximal F-test (PMF) to determine if identified mean shifts are significant (Wang 2008). The PMF test reduces the amount of change points detected when compared to the standard F-test. RHtestsV4 has the option to analyze the time series while using metadata which documents instrumentation changes. In this case, the standard F-test is used, and of the change points

identified, only those supported by reliable metadata are considered significant.

Although the software can be used without a reference series, in many cases it is not recommended (Wang and Feng 2013). For example if a time series has large variations or seasonality it can become more difficult to detect step changes in the data. In the case of significant wave height time series, Gemmrich et al. (2011) suggests running RHtestsV4 with a reliable reference series and specifically uses the Global Reanalysis of Ocean Waves 2000 (GROW2000) as the reference series (www.oceanweather.com), along with metadata from NDBC and MEDS to detect change points.

3.1.2 Zonation

In addition to the statistical tests implemented in RHtestsV4, we implement another technique called "zonation," sometimes referred to as "segmentation" (Swan and Sandilands 1995). Zonation can be implemented in both "local" and "global" procedures to detect anomalies in a data stream. The local procedure centers a window around a data point and only uses the data within the window to determine if the point being analyzed is a change point. The global procedure uses the entire data record when determining if a specific location is a change point. The global procedure is recommended by Swan and Sandilands (1995) if the local procedure is overly sensitive (e.g., identifying more change points than should be expected). If the local procedure identifies a number of change points within reason the global procedure will likely identify too few change points and will not be sensitive enough.

In this study, we use the local zonation procedure. We find that the results from local zonation yield a number of change points that is comparable to prior work (Gemmrich et al. 2011). In local zonation, a window half-width (h) and threshold (D^2_{min}) are defined. To analyze a point in the time series, h-points before the point being analyzed are grouped into one segment, and h-points after the point being analyzed are grouped into a second segment.

The variance of each segment is calculated (s_1^2, s_2^2), and then the pooled variance of both segments together is calculated. Next, the average of both segments is calculated ($\bar{x}_1$, $\bar{x}_2$), and the difference between the averages of the segments is squared. Dividing this value by the pooled variance gives the "Generalized Distance Squared" (Swan and Sandilands 1995) shown in equation 3.2

$$D^2 = 2(\bar{x}_1 - \bar{x}_2)^2 / s_1^2 + s_2^2. \tag{3.2}$$

D^2 exhibits spikes when there are mean shifts between the two segments being analyzed. These spikes or peaks in D^2 can be used to identify the locations of change points within the time series as shown in Fig. 3.1.

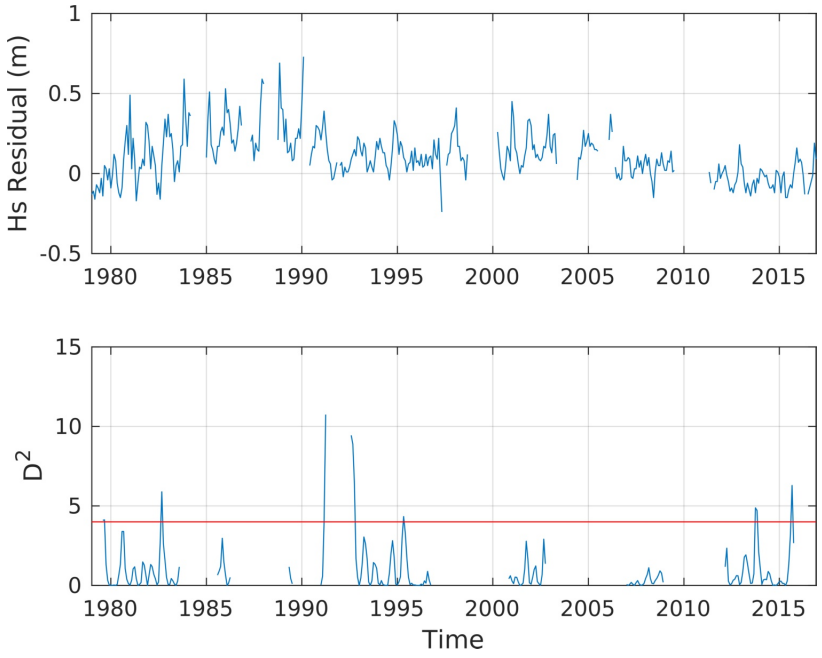

Figure 3.1 Example of how the zonation method identifies change points. (top) Monthly average H_s residuals for buoy WMO46002 and ERA5 hindcast. (bottom) D^2 values calculated with a window half-width of 7 and a threshold D^2 value of 4 (red line).

The number and location of the change points are sensitive to the window half-width, h. A small h detects many erroneous change points. When analyzing a monthly H_s time

Table 3.1 The average number of change point identified for selected half-widths (h) and threshold values (D^2_{min}), per reference series per buoy, (for buoys; WMO46001, WMO46002, WMO46005, WMO42003, and WMO41001).

$h \setminus D^2_{min}$	**2**	**3**	**4**	**6**	**7**	**8**
6				2.70	1.87	1.33
7		3.80	2.20			
8	3.47	1.57				

series with an h only spanning a few months, local zonation often is too sensitive and even transitions in the seasonality are detected rather than changes to buoy configuration. We test a range of half-widths and we find that the minimum window half-width should be at least six months. Alternatively, if h is too large, such as spanning a few years, then the months at the beginning and end of the time series cannot be analyzed. Therefore we set a maximum half-width of twelve months. We then test $6 \leq h \leq 12$ months and find that when $h \geq 10$, the D^2 peaks are significantly reduced which reduces the number of change points identified.

Along with choosing an appropriate h, a minimum threshold value D^2_{min} must be defined to identify the change points. We calibrated local zonation to output a comparable number of change points as RHtestsV4. Note that the specific locations of local zonation and RHtestsV4 are not constrained but only the number of change points. Five NDBC buoys, (WMO46001, WMO46002, WMO46005, WMO42003, and WMO41001), are analyzed using the RHtestsV4 software with six different reference series. For these buoys the average number of change points identified per reference series per buoy is 3.07. For the five buoys the number of change points identified per reference series per buoy when using the zonation technique with different window half-widths h and D^2_{min} threshold parameters are shown in Table 3.1.

Table 3.2 The maximum and minimum number of change points are identified for selected half-widths (h) and threshold values (D^2_{min}), (for buoys; WMO46001, WMO46002, WMO46005, WMO42003, and WMO41001).

$h \setminus D^2_{min}$	**2**	**3**	**4**	**6**	**7**	**8**
6				30, 7	25, 4	18, 1
7		36, 6	20, 3			
8	38, 4	14, 3				

For buoys WMO46001, WMO46002, WMO46005, WMO42003, and WMO41001, RHtestsV4 identifies a maximum and minimum of 21 and 16 change points respectively. We show the maximum number and minimum number of change points identified per buoy with the different local zonation parameters in Table 3.2. The zonation parameters that most closely match the RHtestsV4 results are $h = 7$ and $D^2_{min} = 4$. The average number of change points identified per reference series per buoy for these parameters is 2.20 which is lower than the average from RHtestsV4 which is 3.07. However, the other parameters that have an average closer to RHtestsV4 also have much higher maxima for the number of identified change points per buoy. For RHtestsV4 the maximum number of identified change points per buoy is 21, and for the parameters with higher averages the maximum number of identified change points is 30 or greater.

3.2 Results

3.2.1 RHtestsV4

We show the results from using RHtestsV4 to analyze H_s records for buoy WMO46002 in Fig. 3.2. Appendix C describes the systematic procedure we implemented when applying

RHtestsV4 (Wang and Feng 2013).

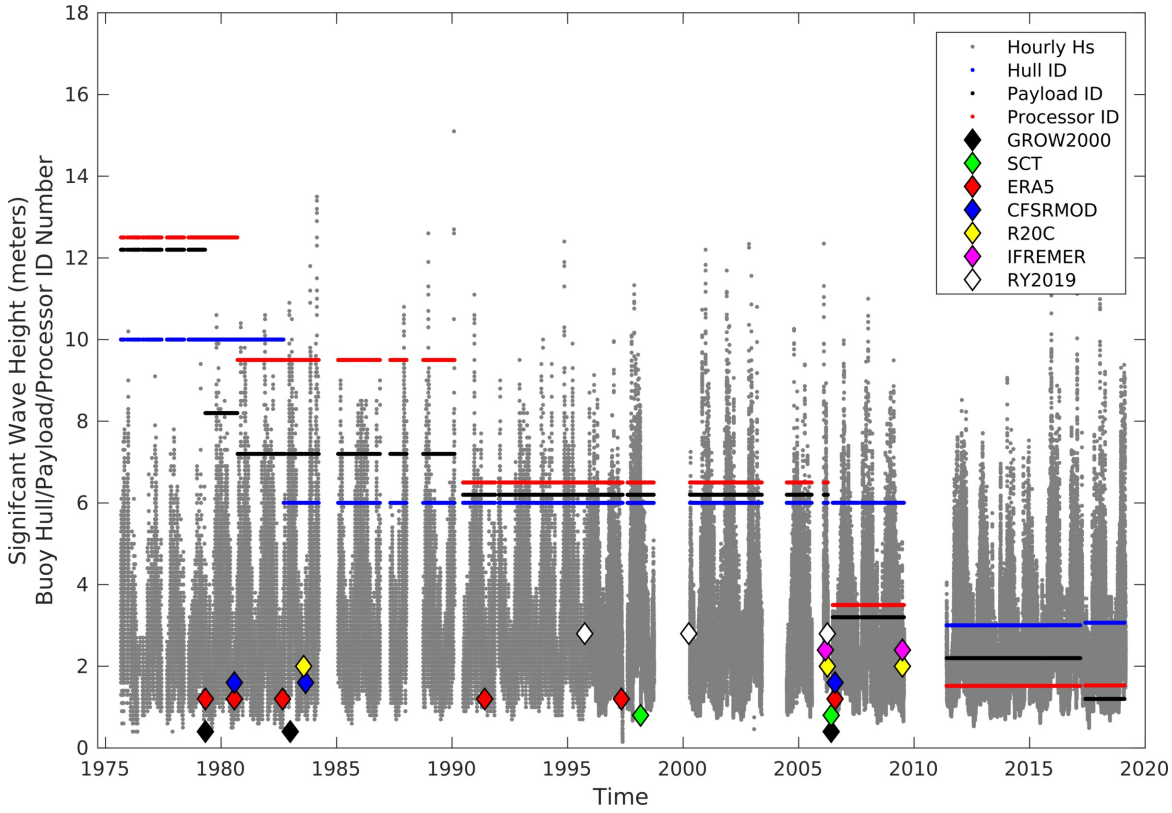

Figure 3.2 Hourly significant wave height observations with change points identified for buoy WMO46002 with different reference series (indicated by diamonds) using RHtestsV4. The black diamonds indicate the dates of the change points identified using the GROW2000 reference series (Gemmrich et al. 2011). Hull, payload, and processor changes are indicated by blue, black, and red lines respectively.

Of the reference series used, four are hindcast data sets and two are altimetry data sets. There is not much agreement in either the number or the location of identified change points between the different reference series. There is agreement between the reference series for the change point identified around 2006. However, this change point is only significant for each of the reference series if all the other change points for each reference series can be accepted as significant. If any change point identified with a specific reference series is determined to not be significant it needs to be removed and the software needs to reanalyze the series to

recalculate the significance of the remaining change points for that reference series. Removal of change points can make neighboring change points not significant because the RHtestsV4 software segments the time series between change points and removing change points changes the lengths and total number of segments being analyzed. For this reason, the significance of one change point is dependent on the significance of the other change points also identified within the time series.

Appendix D contains the results from analyzing buoys WMO46001 and WMO46005 which were similar to the results from WMO46002. The change points identified in the previous study using the GROW2000 reference series (Gemmrich et al. 2011) do not match well with the change points identified using different reference series. Two other buoys were also analyzed using this method, buoy WMO42003 from the Gulf of Mexico and buoy WMO41001 from the north Atlantic. Appendix D also contains the results for these buoys which also had similar results, with little agreement between the different reference series used.

3.2.2 Zonation

The results from using the zonation technique to analyze significant wave height records for buoy WMO46002 are shown in Fig. 3.3. There are no results for the GROW2000 reference series because Gemmrich et al. (2011) did not use the zonation technique. In this case, there is even less agreement between the reference series. The ERA5 reference series detects seven change points, the CFSRDMOD and R20C reference series each detect only one change point, while the IFREMER and RY2019 altimetry data sets both detect zero change points. Appendix D contains the results for the other four buoys.

It should also be noted that many of these change points occur in locations where there are no documented changes to buoy hulls, payloads, or processors. It is possible that other

changes could have occurred at these locations, such as changes to mooring configurations. However, without documentation for these other types of changes it is not possible to attribute the identified change points with changes to buoy configuration. Rather, it appears that the identified change points are more than likely due to differences between the reference series.

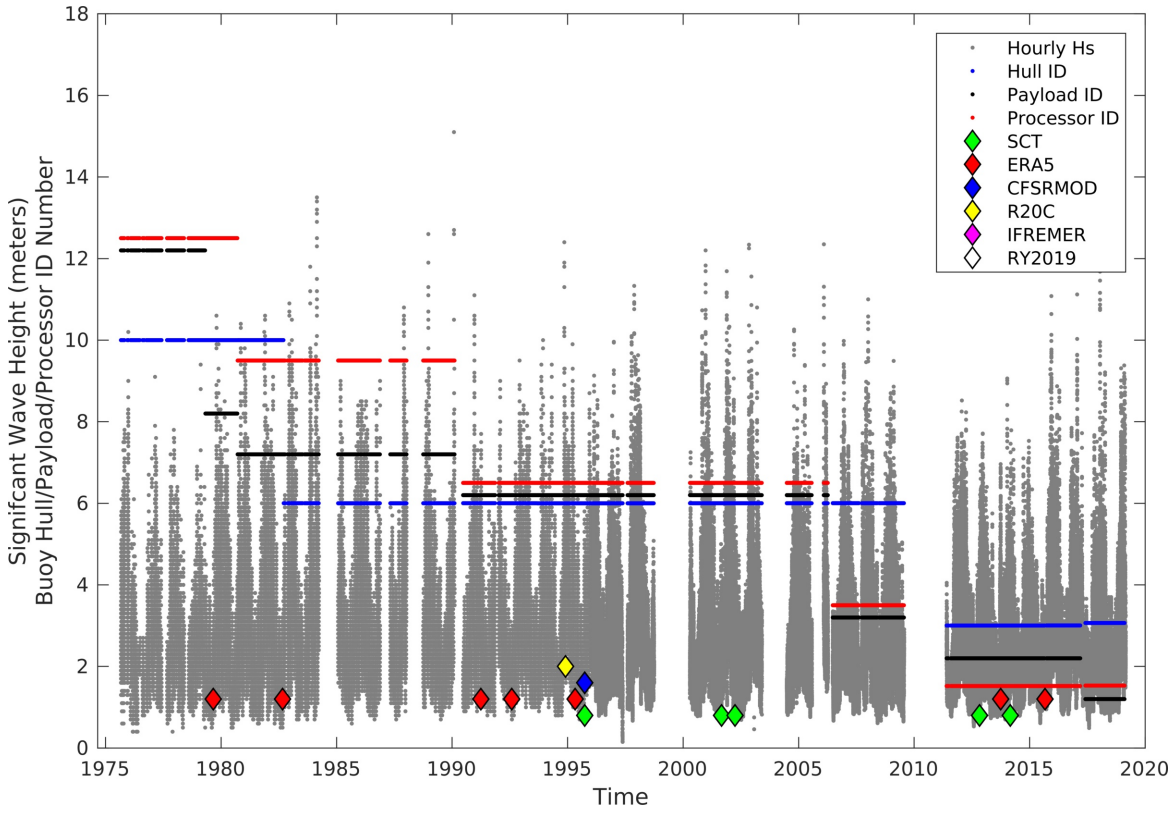

Figure 3.3 Hourly significant wave height observations with change points identified for buoy WMO46002 with different reference series (indicated by diamonds) using the zonation technique. Hull, payload, and processor changes are indicated by blue, black, and red lines respectively.

3.3 Conclusions

We show that both RHtestsV4 and local zonation methods are highly sensitive to the reference series. For some buoys, when using one particular reference series many change points are identified while no change points are identified when using another reference series. One likely reason for the differences in the number and locations of change points identified is that the magnitudes of the step changes within the data are either very small or perhaps even insignificant. Also, there are known differences between each of the reference series used and there is not one specific reference series that can be said to be the most reliable, as they each of their own unique limitations. The differences in how the hindcast products are created, as well as the differences in the wind forcing leads to different estimates of H_s especially in extreme sea states (Stopa 2018). In regards to the altimetry datasets, although the same satellite platforms are used, differences in data processing techniques as well as in quality control methods create significant differences between altimeter products (Timmermans et al. 2020). As a result, none of these references series are sufficiently reliable to identify change points. In the absence of a reliable reference series, neither RHtestsV4 nor local zonation are effective.

A conclusion reached from the previous study which is still likely valid is that the specific WSA processor causes a step-change (Gemmrich et al. 2011). However, this was not only identified through the RHtestsV3 software, but also by simply removing data with this processor from the time series (Gemmrich et al. 2011). Excluding data before 1980 eliminated the spurious trends that had been reported in previous studies (Ruggiero et al. 2010). Along with this, it would intuitively be expected that this processor would cause a significant bias in H_s, as it limited individual wave height measurements to $\pm$11 m, which was later increased to $\pm$20 m in subsequent processors (Gemmrich et al. 2011). This can even be observed

visually in the hourly time series in Fig. 3.3. Before 1980 there are no significant wave height measurements greater than 11 m, but throughout the rest of the time series there are many significant wave height measurements greater than 12 m and some greater than 14 m. The impact of the WSA processor is likely greatest in regions that experience extreme sea states because in regions with relatively smaller waves the ± 11 m wave height limit will rarely be reached. However, there is no clear evidence that suggests that other changes to buoy configurations lead to significant biases in the data records.

Chapter 4

Observational Uncertainties of Altimeters and Buoys

4.1 Background: Multi-Decadal Trends

Young et al. (2011) reports regional H_s trends in mean, 90th percentile, and 99th percentile from 1985 to 2008 using satellite altimetry. In general, they find the majority of the global ocean has increasing trends in the 90th percentile which was corroborated with a more recent study using data from 1985 to 2018 (Young and Ribal 2019). Altimeters suffer from low sampling so estimating trends of the 99th percentile may not be very accurate and even estimating trends of the 90th percentile may not be appropriate.

The NDBC network specifies an H_s tolerance of ± 0.2 m for most payloads (N. NDBC 2017). This tolerance range is large, especially when compared to estimated trends which are on the order of centimeters per year. However, buoys do not suffer from the same sampling limitations of altimeters so computing trends of the 90th percentile and 99th percentile from buoy data records is more reasonable. With that said, using a hindcast is the best way to address issues of sampling.

An attempt was made to correct buoy data records using RHtestsV3 (Gemmrich et al. 2011). However, in the absence of a reliable reference series the results of this method are not repeatable using RHtestsV4 or local zonation (e.g., Chapter 3). Therefore, neither of these methods are an appropriate way to correct buoy data records. Since both methods

to identify change points are highly dependent on the reference time series, we use another approach to estimate uncertainties in observational H_s datasets.

One way to understand the impact of changes to buoy configurations on significant wave height observations is to compare the observations with altimetry observations which have been co-located in time and space, and specifically finding the residuals between the observations. The residuals between the buoy data sets and the altimetry data sets can be understood as the "errors" from one data set relative to another. For the buoy these errors are a result of the limited precision of the buoy itself as well as the accuracy of the buoy which can be impacted by changes to the buoy configuration.

Altimetry datasets have a high level of consistency through time due to cross-validation that occurs when there are co-locations in space and time between two altimeter platforms (Young et al. 2017), which allows for any errors in one altimeter to be identified and corrected. So by comparing buoy data, which has known inconsistencies through time, to altimetry data the residuals between the two datasets can show if there are any time periods where buoys have any significant biases in the data records. We propagate residuals from co-located altimeter-buoy time series onto the original buoy time series in order to create synthetic time series. By creating many iterations of synthetic time series and calculating trends for the synthetic time series, the range of the trends indicates the variation in buoy trends that are induced by buoy errors.

The altimeter platforms are individually calibrated by Young et al. (2017) against all of the data from NDBC buoys 50 km offshore during the specific period of altimeter deployment. As a result, the altimeter data set is not completely independent of the buoys that were used for the calibration. However, because the altimetry data set was calibrated against the aggregate buoy data, the direct influence from an individual buoy is minimal. In Table A.1 in Appendix A, we quantify the percentage of data used to calibrate each altimeter

from each individual buoy relative to the total amount of data used in calibration. After this calibration step Young et al. (2017) use co-located data from buoys outside of the NDBC network collected by ECMWF to validate the altimeter calibration. The altimeters are further cross-validated by Young et al. (2017) when two altimeters observe the same location at the same time. This procedure further reduces the dependence of an altimeter platform on the impacts of changes to buoy configuration made to a single buoy.

4.1.1 Differences in Altimeter and Buoy Observations

Buoy measurements as well as altimeter measurements are both estimations of sea state at a specific location in space and time. In regards to individual altimeter measurements, there is also associated uncertainty. The differences in how the raw data from altimeters is processed leads to significant differences in estimations of significant wave height. As a result, for each co-located observation, neither buoy nor altimeter can be said to be the "true" significant wave height value for that specific sea state. Rather, both values are "realizations" of the sea state, each with their own associated uncertainty.

Along with the spatial and temporal constraints for co-locating altimetry and buoy observations, one other criterion that is used in the co-location process is a measure of the along track variability, also used in previous studies (Young et al. 2017), defined as $\sigma(H_s)/\bar{H}_s$, where $\sigma(H_s)$ is the standard deviation of the significant wave height measurements and $\bar{H}_s$ is the mean. Altimeter data with along track variability greater than 0.2 are excluded, along with data outside of the spatial and temporal constraints. From the co-located data, the residuals between the buoy measurements and the altimeter measurements can be calculated. These residuals are an indication of the uncertainty between the two measurement techniques. The residuals from buoy WMO46002 and the co-located altimetry data are shown in Fig. 4.1 (a).

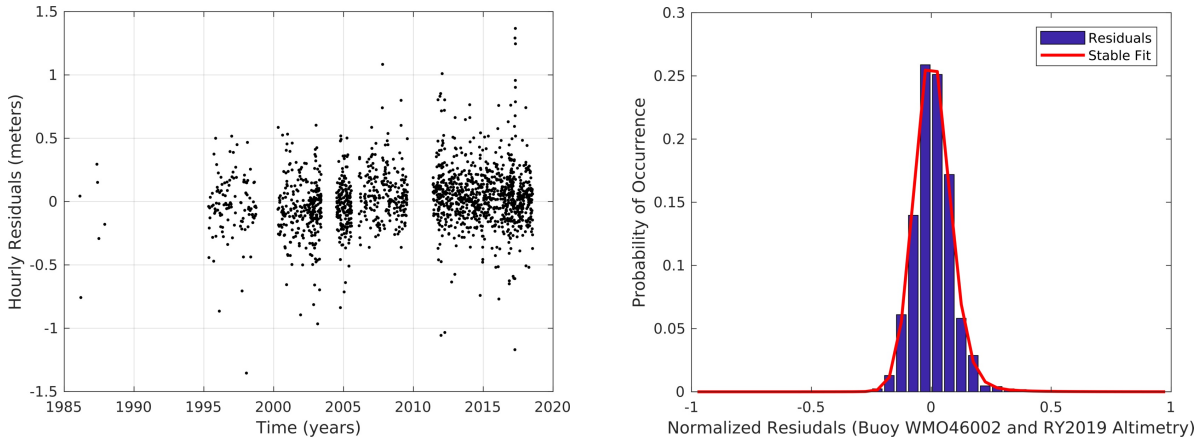

(a) Hourly Residuals **(b)** Probability Distribution with Stable Fit

Figure 4.1 (a) Hourly residuals of co-located significant wave height observations from buoy WMO46002 and RY2019 altimetry. (b) Stable distribution fit (red) for probability distribution of residuals from buoy WMO46002 and RY2019 altimetry (blue).

In Fig. 4.1 (b) we show the probability distribution of the normalized residuals. The probability distribution can be fit with the Stable Distribution, which uses two shape parameters (alpha and beta), one scale parameter (gamma), and one location parameter (delta). To fit a stable distribution to the probability distribution of the residuals the parameters are as follows; alpha = 1.9, beta = 0.9, gamma = 0.05, and delta = 0.0007. We find that the values for alpha and beta can be set to constant values while fitting the residuals well for other buoys. The value for gamma can be approximated as proportional to the standard deviation of the residuals and the value for delta can be approximated as the median of the residuals. It should be noted that the gamma parameter is very important and if this value is not accurate the fit of the residuals will be poor. The number of monthly co-locations is limited, with many months having less than five co-locations. For this reason an accurate approximation of the standard deviation cannot be obtained consistently on a monthly basis. This significantly reduces the accuracy of the fit on a monthly basis. Grouping the co-locations based on buoy configuration from metadata would result in a more accurate

estimation of the standard deviation due to an increased amount of co-locations within each buoy configuration group. However, this would limit the technique to only those buoys with comprehensive metadata. For this reason we consider all of the residuals throughout the entire time series rather than considering residuals on a monthly basis or based on buoy configuration.

4.2 Synthetic Time Series

One thing the residuals do indicate is a range of values, which give an idea of the uncertainty of the measured value. For each buoy measurement, the actual value for significant wave height is likely somewhere within the range of the residuals. Adding a residual value chosen at random from the entire set of co-located residuals is a way to create a "synthetic" observation. If this is done many times, the "true" value will likely lie within the range of "synthetic" values. Also, the synthetic values can be thought of as measurements that "could have been recorded" based on the range of the uncertainty between buoy and altimeter. Randomly applying a residual to every value in the original buoy time series creates a synthetic time series based on observed uncertainty between buoy and altimeter measurements which can be seen in Fig. 4.2. This synthetic time series is bounded by the range of the residuals of the co-located altimetry-buoy time series.

Equations 4.1 shows how the residuals are calculated, with i representing values from one through the length of the co-located buoy time series, Ac_i representing the co-located altimeter time series, Bc_i representing the co-located buoy time series, and Rc_i representing the co-located altimeter-buoy residuals.

$$Rc_i = Ac_i - Bc_i \tag{4.1}$$

Equations 4.2 shows how the residuals are normalized, with nRc_i representing the normalized

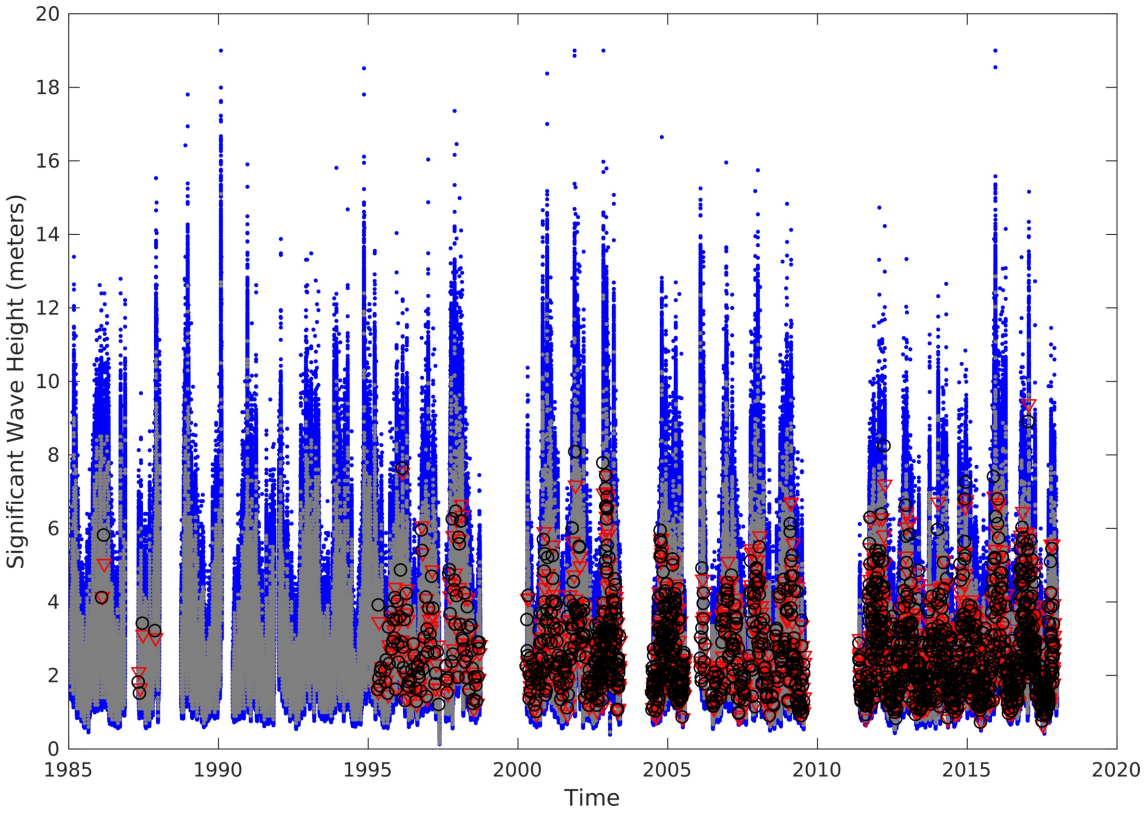

Figure 4.2 Hourly significant wave height observations for buoy WMO46002 (grey), 1000 synthetic observations (blue), co-located RY2019 altimeter observations (red triangles), and co-located buoy observations (black circles).

co-located altimeter-buoy residuals.

$$nRc_i = Rc_i \div Bc_i \tag{4.2}$$

Equation 4.3 shows how the synthetic time series are created, with j representing values from one through the length of the original buoy time series, S_j representing the synthetic time series, B_j representing the original buoy time series, and nRc_r representing a normalized co-located residual chosen at random.

$$S_j = B_j + (nRc_r \times B_j) \tag{4.3}$$

It should be noted that if a value within the synthetic time series exceeds 19 m, that value

is set to 19 m, as values greater are not realistic for significant wave height. Similarly if a value within the synthetic time series is less than 0.1 m, that value is set to 0.1 m.

For some of the residuals it is clear that they are outliers. This could potentially occur if a buoy battery is low causing the measurements to become very inaccurate (which is not consistently recorded in metadata records), among other reasons. Outliers can also occur due to issues with altimeters, as instantaneous measurements from altimeters are known to at times be erroneous (Timmermans et al. 2020). In order to exclude these outliers, for significant wave heights greater than one meter, residual values greater than 100 percent of the observed value are removed. The remaining residuals are used to create the synthetic time series as follows:

- The residuals, calculated as shown in equation 4.1, are normalized by dividing by the value of the observed significant wave height measured by the buoy, as shown in equation 4.2.
- From the normalized residuals, one is randomly chosen and applied to each individual observation of the buoy time series, as shown in equation 4.3.
- The normalized residual is multiplied by the buoy significant wave height value that it is being applied to and then it is added to that buoy significant wave height observation, as shown in 4.3.
- This is done for all the observations within the time series after 1985, because this is when the first altimeter observations begin.

From the synthetic time series, yearly statistics such as the mean can be calculated as shown in Fig. 4.3 (a). We set the criteria to determine whether there is enough data present to calculate statistics for each year as follows:

- There must be a minimum of six months with at least one observation per month in order to calculate yearly statistics.
- Months without observations cannot occur consecutively.
- Months without observations cannot occur on the first and last month of the year simultaneously.

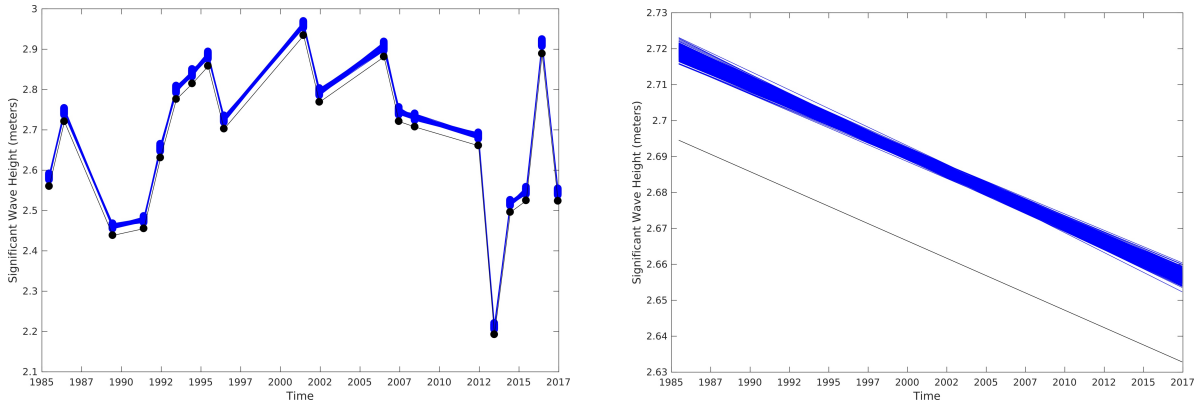

(a) Annual Averages **(b)** Trends of Annual Averages

Figure 4.3 (a) Annual averages for buoy WMO46002 time series (black) and 1000 synthetic time series (blue). (b) Trends of buoy annual averages (black) and 1000 synthetic annual averages (blue).

These criteria are set in order to ensure that the data is reasonably representative of a full year. For buoys in regions that have large waves during winter, missing three months during a winter season would greatly impact the yearly statistics and would bias them lower for that year. Alternatively, missing three months during summer could bias the statistics higher. However, when setting criteria for calculating yearly statistics it is also important to make sure that the criteria is not too exclusive, otherwise there will only be a few years that meet the criteria to be considered when calculating yearly statistics.

Creating yearly statistics from years that have enough data such that they are a reasonable representation of a full year increases the confidence in any trends estimated from

those yearly statistics. In this study, we estimate trends starting no earlier than from 1985 because this is when satellite altimetry data is first available which is necessary to create the synthetic time series. As the synthetic time series are generated by randomly choosing residuals to apply to the buoy observations, it is of interest to generate many of these synthetic time series and then to calculate trends for each synthetic time series. For this study we generate one thousand synthetic time series for each buoy location in order to have a wide range of synthetic time series while also considering computational limitations. The minimum and maximum trends from the synthetic time series indicate the uncertainty range for the buoy trends estimated based on the combined buoy and altimeter errors and can be seen in Fig. 4.3 (b).

4.3 Trends and Uncertainty

The first set of results shown in Fig. 4.4 compare trends of the original buoy time series with trends of the synthetic time series, only using data after 1985. The buoy time series and the synthetic time series have the same sampling so this allows for direct comparisons of buoy and synthetic trends at specific buoy locations. It should also be noted that regional trends cannot be accurately established from this first set of results because each buoy location has a unique deployment so the time periods at the different buoy locations are not comparable. Further results will focus on fixed time periods. The objective in this first set of results is to show how the trends from the buoy time series compare with the trends from the synthetic time series.

For the buoy trends, the trend plotted is the slope estimated through linear regression. We obtain the 95% confidence interval of the slope, which is estimated through linear regression. This calculation specifies the confidence range of the trend estimates based on the values of

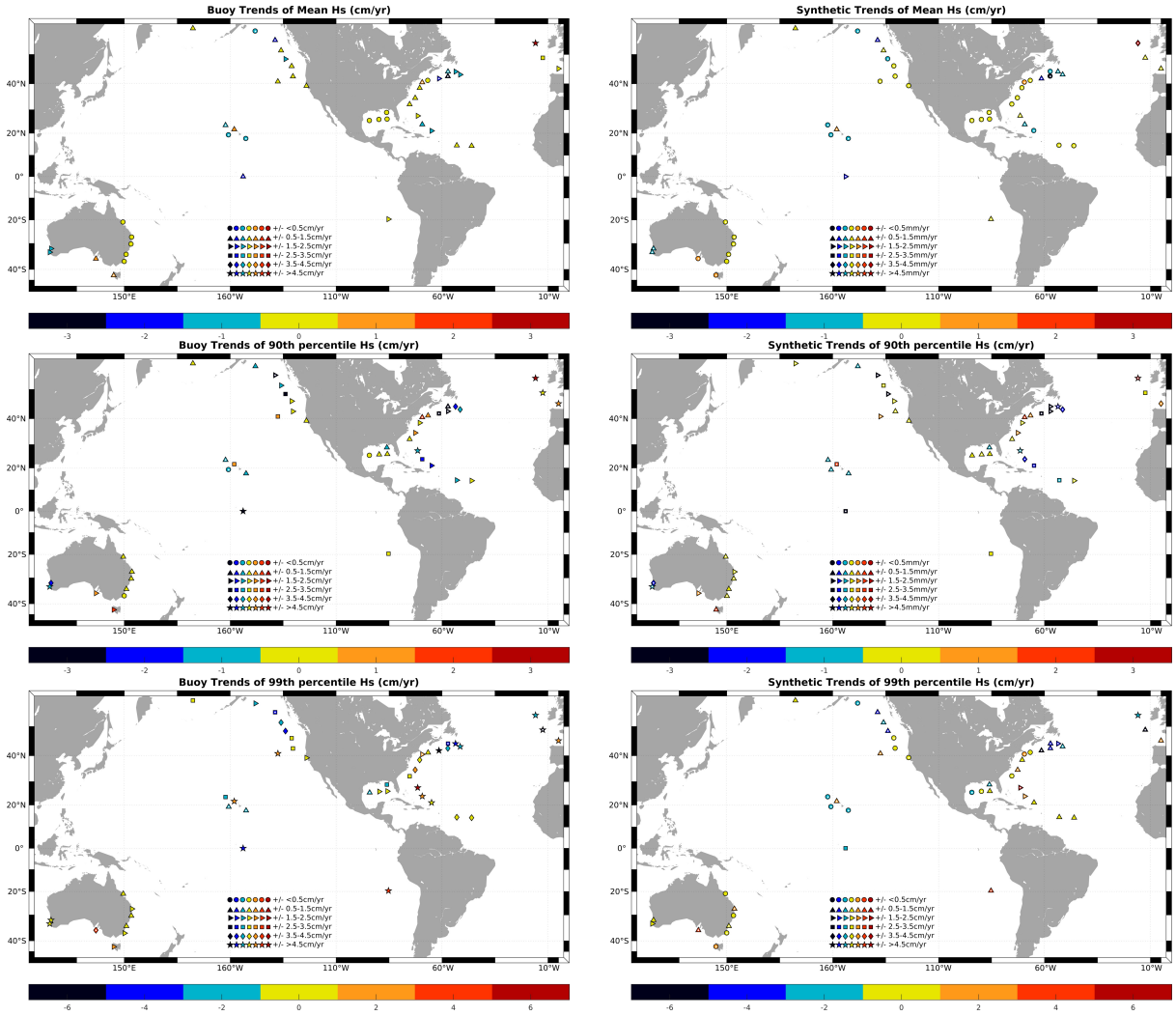

Figure 4.4 Buoy trends (left) and synthetic trends (right) of annual mean (top), 90th percentile (middle), and 99th percentile (bottom) significant wave height for different time periods after 1985. Color bar represents magnitude of trends in centimeter per year. White dot within marker indicates that confidence interval/trend range does not cross zero.

the yearly statistics that we use to compute the trends. We use this confidence interval to determine if the the calculated trends are significant. If the confidence interval is all positive or all negative this indicates that the estimated trend is significant. When the confidence interval is either all positive or all negative this is designated by a white dot within the plotted marker.

For the synthetic trends, the trend plotted is the mean of the one thousand trends calculated for each buoy location. The minimum and maximum trends are also identified and if they are both positive or both negative this is noted and shows that even with the errors propagated onto the time series the sign of the trend remains constant. When the trends are either all positive or all negative this is designated by a white dot within the plotted marker.

Trends are shown for annual mean, 90th percentile, and 99th percentile significant wave height in Fig. 4.4. From these plots it can be seen that there is very good agreement between the magnitudes of the buoy and synthetic mean trends. The magnitudes of the buoy and synthetic 90th percentile trends also have good agreement. And even at the 99th percentile the magnitudes of the buoy and synthetic trends have good agreement.

For the buoy trends, few of the trends are designated as significant at the 95% confidence interval. This can be expected because at most buoy locations the range of the confidence interval is on the order of centimeters per year and the buoy trends are also on the order of centimeters per year. The range of the confidence interval is indicated by the different symbols shown on the plots. It should also be noted that the range of the confidence interval at most buoy locations is smallest for the mean trends and largest for the 99th percentile trends.

For the mean and 90th percentile synthetic trends, at most of the locations the minimum and maximum trends are either both positive or both negative. The reason for this is because most of the synthetic trends are on the order centimeters per year, while the trend ranges are on the order of millimeters per year. This shows that propagating the altimeter-buoy residuals to create the synthetic time series has a minimal impact on the overall mean and 90th percentile trends. This is further evidence that most changes to buoy configurations have a minimal impact on overall buoy trends, as the sign of the buoy trends generally remain

the same for all of the one thousand estimated trends from the synthetic time series at each buoy location. However, at the 99th percentile the trend ranges increase significantly and are on the order of centimeters per year. This results in more locations where the minimum and maximum synthetic trends are not both positive or both negative. The range from the maximum to the minimum synthetic trends is indicated by the different symbols shown on the plots. This shows that propagating the altimeter-buoy residuals to create the synthetic time series has a much larger impact on the overall 99th percentile trends. Based on these findings, we only estimate mean and 90th percentile trends when examining regions over specific time periods.

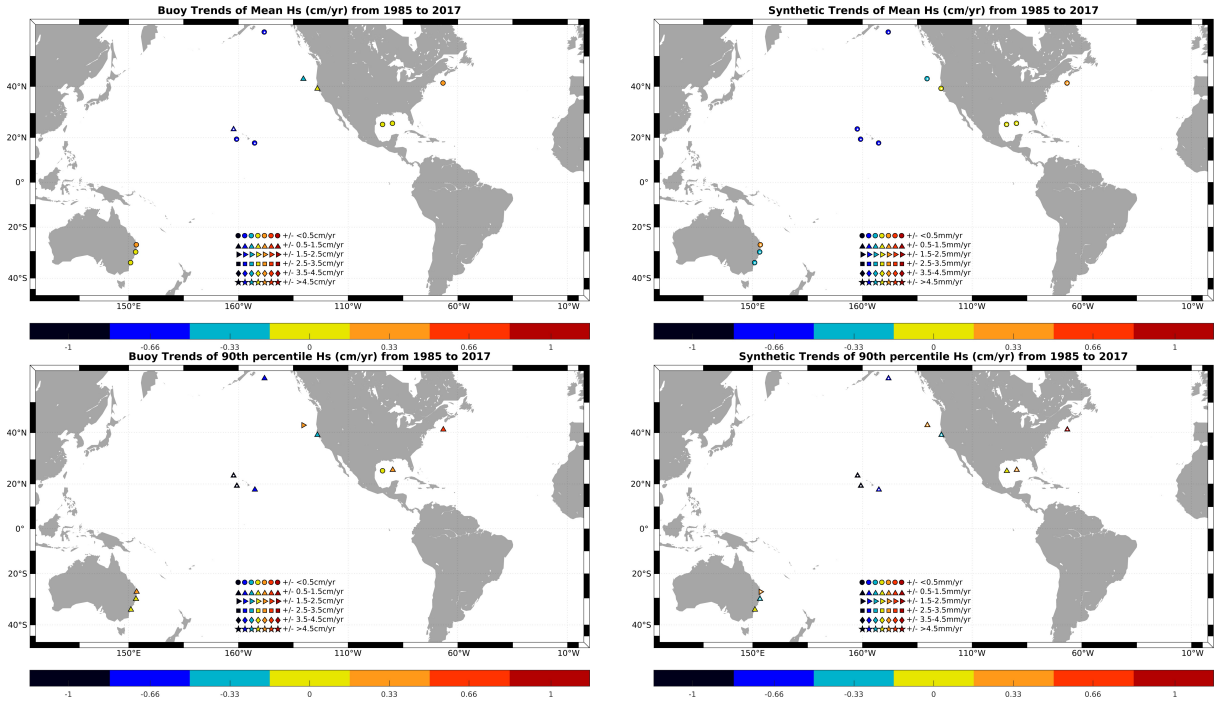

Figure 4.5 Buoy trends (left) and synthetic trends (right) of annual mean (top) and 90th percentile (bottom) significant wave height from 1985 to 2017. Color bar represents magnitude of trends in centimeter per year. White dot within marker indicates that confidence interval/trend range does not cross zero.

The following sets of results are for the buoy time series and the synthetic time series over specific time periods. Only data within the specified time period are used, and because the

synthetic time series are created from the buoy time series the trends for buoy and synthetic time series are both based on the buoy sampling. This allows for assessments to be made of regional trends over the specified time periods.

Trends are shown from 1985 to 2017 for annual mean and annual 90th percentile significant wave height in Fig. 4.5. For the buoys around Hawai'i trends are decreasing with the magnitudes of the trends increasing for the higher percentiles, and most of them are designated as significant. In the northeast Pacific the trends are mostly decreasing, although most of them are not identified as significant. The Gulf of Mexico shows neutral trends. The Australian east coast shows a combination of increasing and decreasing trends with none identified as significant.

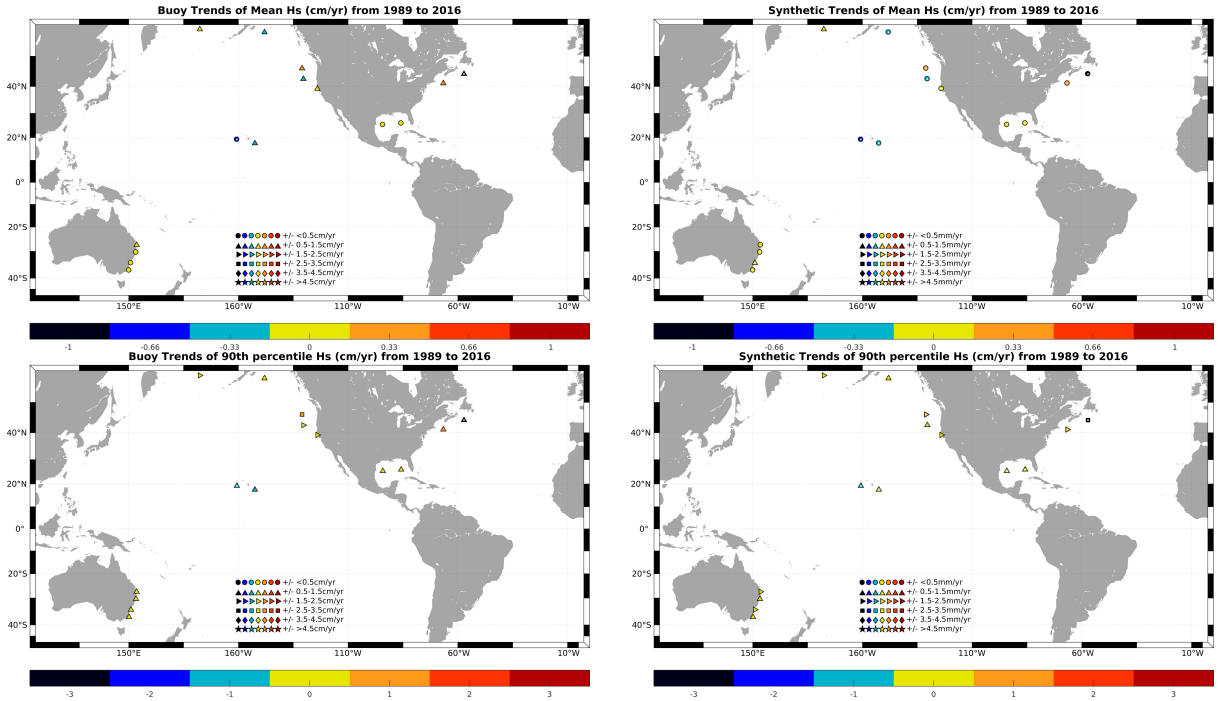

Figure 4.6 Buoy trends (left) and synthetic trends (right) of annual mean (top) and 90th percentile (bottom) significant wave height from 1989 to 2016. Color bar represents magnitude of trends in centimeter per year. White dot within marker indicates that confidence interval/trend range does not cross zero.

Trends are shown from 1989 to 2016 for annual mean and annual 90th percentile signifi-

cant wave height in Fig. 4.6. The buoys around Hawai'i again show decreasing trends. The buoys in the northeast Pacific now show both increasing and decreasing trends, with none of the trends being identified as significant. Trends in the Gulf of Mexico are again neutral. The northwest Atlantic shows increasing and decreasing trends but with only the decreasing trends identified as significant. The Australian east coast shows neutral trends.

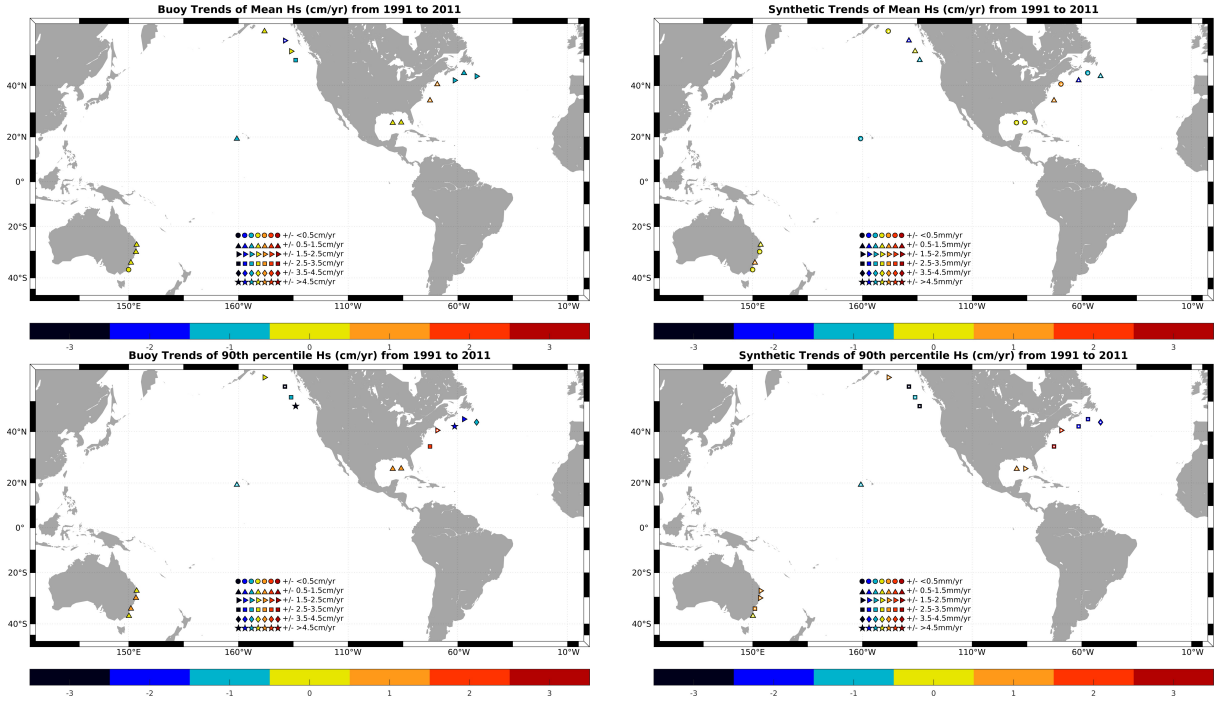

Figure 4.7 Buoy trends (left) and synthetic trends (right) of annual mean (top) and 90th percentile (bottom) significant wave height from 1991 to 2011. Color bar represents magnitude of trends in centimeter per year. White dot within marker indicates that confidence interval/trend range does not cross zero.

Trends are shown from 1991 to 2011 for annual mean and annual 90th percentile significant wave height in Fig. 4.7. The one buoy during this time period around Hawai'i again shows a decreasing trend which is identified as significant for the 90th percentile. The northeast Pacific shows generally decreasing trends with one buoy being identified as significant for the mean and 90th percentile. The Gulf of Mexico shows increasing trends at the 90th percentile but none of the trends are identified as significant. Along the US east

coast there are increasing trends with locations being identified as significant for the mean and 90th percentiles. This is contrast with the Canadian east coast which shows decreasing trends, however these are not identified as significant. The Australia east coast shows some increasing trends but none of them are identified as significant.

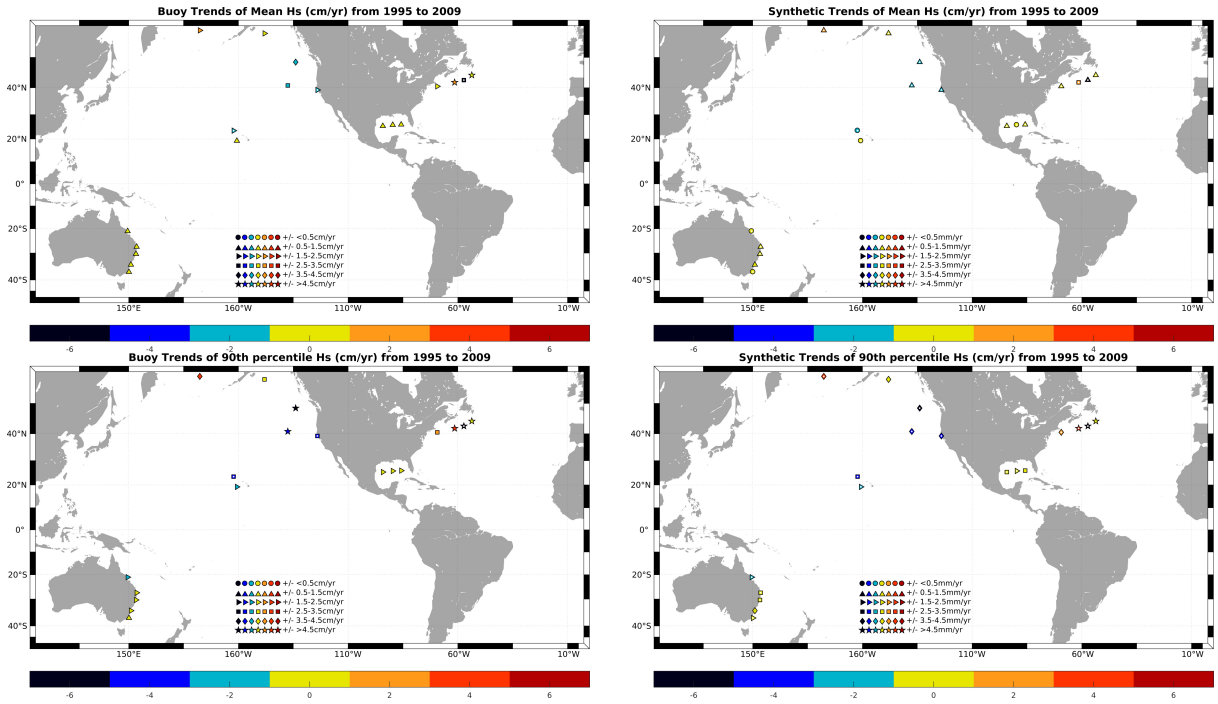

Figure 4.8 Buoy trends (left) and synthetic trends (right) of annual mean (top) and 90th percentile (bottom) significant wave height from 1995 to 2009. Color bar represents magnitude of trends in centimeter per year. White dot within marker indicates that confidence interval/trend range does not cross zero.

Trends are shown from 1995 to 2009 for annual mean and annual 90th percentile significant wave height in Fig. 4.8. Again, the buoys around Hawai'i show decreasing trends with two being identified as significant. The northeast Pacific shows mostly decreasing trends with the only significant trends being identified off the coast of California for the mean and 90th percentile. The Gulf of Mexico shows neutral trends. The northwest Atlantic shows increasing and decreasing trends with one decreasing trend identified as significant for the mean and 90th percentiles. The Australian east coast shows mostly neutral trends.

4.4 Conclusions

The results from the buoy and synthetic time series show that the synthetic time series are comparable to the buoy time series. The agreement in the magnitudes of the trends between the synthetic time series and the buoy time series is good for the annual mean, 90th percentile, and 99th percentile trends. Also, the synthetic trends have relatively small ranges between the maximum and minimum trends, on the order of millimeters per year, for the annual mean and 90th percentile trends, while the trends themselves are on the order of centimeters per year. However, for the synthetic annual 99th percentile trends the range between the maximum and minimum trends is on the order of centimeters per year.

The results for the regional trends showed limited buoy locations with significant trends. However, from trends that were identified as significant, buoy locations around Hawai‘i consistently show decreasing trends. In the northeast Pacific not many trends are identified as significant, but those that are significant are decreasing. From the Gulf of Mexico buoys most of the trends are neutral. The US and Canadian east coasts show a mix of trends with some significant increasing as well as decreasing trends. None of the buoys located around Australia had trends identified as significant.

Chapter 5

Discussion, Conclusions, and Outlook

5.1 Discussion

Of the observational techniques used to measure significant wave height, buoys have many advantages. One aspect of buoys that cannot be understated is that buoys are an in situ data source. While satellites have also been shown to be very effective, especially at providing global measurements, they need buoy data in order to correctly calibrate the raw altimetry data (Young et al. 2017). Along with this, even with multiple satellite platforms in orbit, the sampling of a specific location by altimeters will always be limited, with altimeter sampling being orders of magnitude less than the sampling of buoys. While the use of hindcasts to estimate significant wave height has the advantage of high sampling rates (subject to computational resources), differences in how the hindcasts are generated can lead to very different results (Stopa 2018).

As with any measurement technique, buoys come with inherent uncertainties. We show that these uncertainties have a minimal impact on trends of annual mean and 90th percentile significant wave height. After propagating the altimeter-buoy residuals onto the buoy time series to create synthetic time series the range of the synthetic trends is on the order of millimeters per year while the trends themselves are on the order centimeters per year, for the annual mean and 90th percentile. However, the range of the synthetic trends is on the order of centimeters per year for the annual 99th percentile, so there is less confidence in trends estimated at the 99th percentile. It should also be reiterated that other observational

techniques are not free of uncertainties. The different processing techniques used for the raw data from altimeters has led to significant differences in the final altimeter products (Timmermans et al. 2020). For this reason buoys have been and will remain an indispensable ocean observing technology.

With that said, the importance of documenting and storing comprehensive metadata records for buoy configurations cannot be understated. While we show that the majority of the changes to buoy configurations have minimal impacts on overall buoy annual mean and 90th percentile trends, initial changes to buoy processors did in fact have a very large impact on the overall trends (Gemmrich et al. 2011). Careful documentation of metadata allowed that specific change to be identified as very significant while also allowing other changes to buoy configurations to be identified as much less significant. As buoy technology continues to evolve there is always the potential for a new buoy configuration to significantly impact overall buoy trends. However, by making sure that any and all new changes to buoy configurations are carefully documented, if any new configurations do in fact cause significant biases these data can be removed from the records without sacrificing the entire time series.

Although changes to buoy configurations can lead to inconsistencies within the data records, we show that these inconsistencies have a minimal effect on trends estimated from the time series. It is important to recognize that initial buoy processors limited wave height measurements to ± 11 m, which after only a few years was increased to ± 20 m (Gemmrich et al. 2011). This has a clear impact on trends as would be expected, and these initial wave records are biased significantly lower due to these processing limitations.

In a recent study buoy WMO46006 is analyzed, shown in Fig. 5.1 (Timmermans et al. 2020), and the question is posed as to why trends shift from positive to negative depending on where the data record begins. For buoy WMO46006 these trends are clearly affected by this processing limitation (in this specific case NDBC buoy 46006 uses a PEB payload and

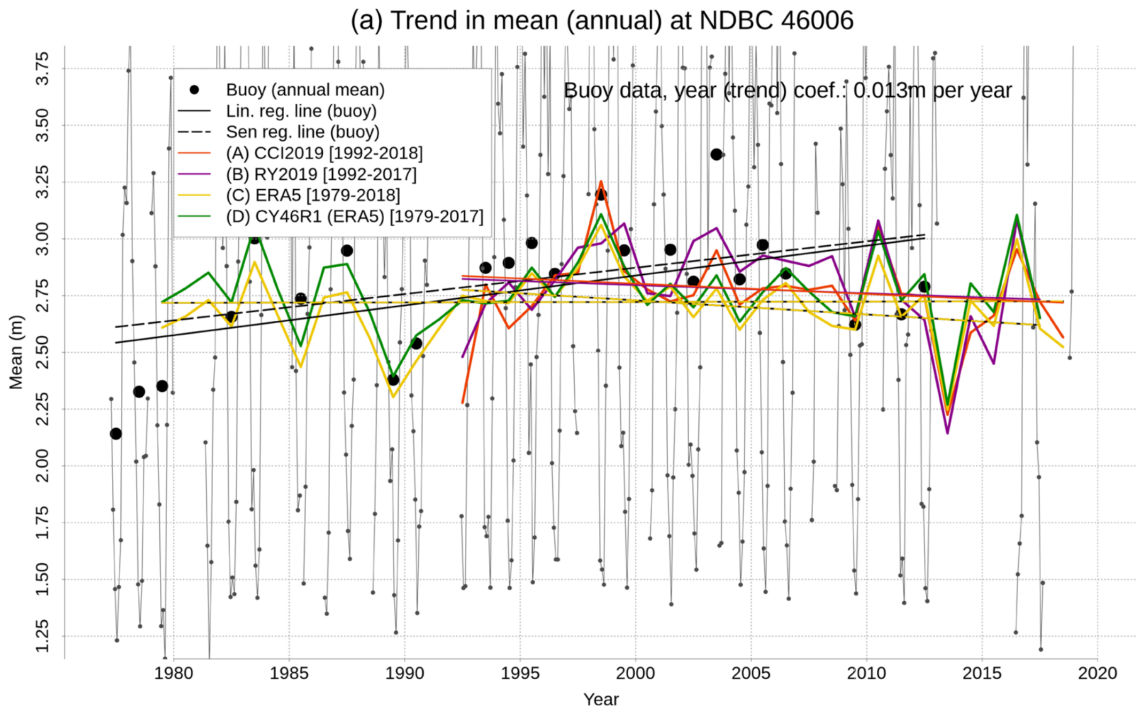

Figure 5.1 Reprint of "Trends in mean (annual) at NDBC 46006" (Timmermans et al. 2020)

a WSA processor), and the first three annual averages can almost visually be identified as outliers. By removing the three initial outliers the trends are corrected. This same conclusion is made in previous work by showing that rather than using RHtestsV3 to correct the time series, simply removing these first few years of biased data achieves the same overall results in trends (Gemmrich et al. 2011).

The method of using synthetic time series to quantify uncertainty addresses two known issues. Firstly, this method limits data records to those that occur within the satellite era. So by excluding data before 1985, data with a low bias due to processing limitations are no longer included in the time series. Secondly, the impact of any other changes to buoy configurations are better understood by randomly propagating the altimeter-buoy residuals on the buoy time series. While other changes to buoy configuration undoubtedly have some

effect, that effect is shown to be quite subtle (particularly when compared to the impact the processing limitation had on early buoy records). This should allow trends estimated from buoy records to be viewed with greater confidence.

With this in mind, it is of interest to compare the synthetic trends to trends from recent studies which use altimeter data records (Young and Ribal 2019). In order to compare trends to previous studies using altimetry it is important to ensure that the trends are being estimated over the same time period. However, with data unavailable for Australian buoys beyond 2017 the synthetic trends are estimated from 1985 to 2017, while altimetry trends are estimated from 1985 to 2018. It should also be noted that in previous studies altimetry trends are estimated using the seasonal Mann-Kendall test (Young and Ribal 2019).

The synthetic trends are estimated using linear regression and although the co-located altimeter-buoy residuals follow a stable distribution, it is important that the errors from the estimated trends obtained through linear regression follow a normal distribution. We preform a chi-square goodness of fit test on the errors from the trend estimated for buoy WMO46002 at the 99% significance level as well as at the 1% significance level, and in both cases we cannot reject the null hypothesis (that the errors are a random sample from a normal distribution).

In Fig. 5.2 it can be seen that altimetry and synthetic annual mean trends are decreasing around Hawai‘i, mostly decreasing in the northeast Pacific, increasing in the northwest Atlantic and neutral in the Gulf of Mexico. The Australian east coast shows a mix of increasing and decreasing for synthetic trends, but trends for altimetry are a mix of increasing and neutral.

For the annual 90th percentile trends altimetry and synthetic trends are a mix of increasing and decreasing in the northeast Pacific. The trends are increasing in northwest Atlantic and a mix of increasing and neutral in the Gulf of Mexico. Altimetry and synthetic trends

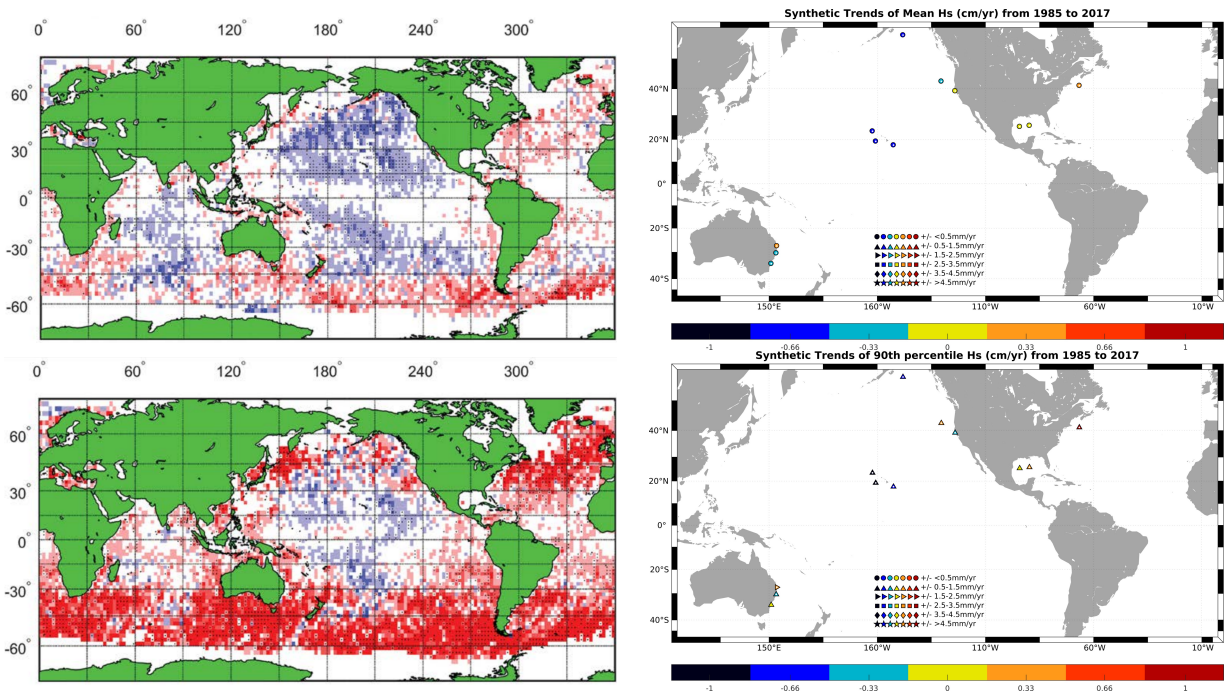

Figure 5.2 Altimeter trends (left) and synthetic trends (right) of annual mean (top) and 90th percentile (bottom) significant wave height from 1985 to 2018 for altimetry trends and from 1985 to 2017 for synthetic trends. The altimetry trends are reprints of "Altimeter Hs mean trend (1985 - 2018) [cm/yr]" (Young and Ribal 2019). The color scale if from -1 (cm/yr) (dark blue) to 1 (cm/yr) (dark red).

are not consistent around Hawai'i, with altimetry showing mostly neutral trends while synthetic trends are decreasing. Also, along the Australian east coast altimetry shows increasing trends while synthetic trends are a mix of increasing and decreasing.

There is stronger agreement between altimetry and synthetic annual mean trends than there is between annual 90th percentile trends. This is likely due to the fact that the synthetic trends are based on the buoy sampling, which is orders of magnitudes greater than the sampling for altimetry. The low sampling of altimetry may make it more difficult to accurately estimate trends in the higher percentiles because those statistics are based off of limited observations.

5.2 Conclusions

The results from chapter three show that neither the RHtestsV4 software nor the zonation technique are able to reliably identify change points in buoy data records of significant wave height due to the lack of a highly accurate reference time series, answering question one from the chapter one. While previous studies did identify that early buoy processors were inducing a low bias on the observations, this was identified not only through RHtestsV4, but also by simply removing that early data from the beginning of the time series (Gemmrich et al. 2011).

Table 5.1 shows the trends from Table 1.1 from chapter one, but with the inclusion of the trends estimated from the synthetic time series. It can be seen that the trends from the synthetic time series are of the same magnitudes as the trends calculated by Gemmrich et al. (2011). However, we find the trend of buoy WMO46005 to be negative rather than positive.

Aside from the change in buoy configuration which caused a significant low bias, there are no other documented changes to buoy configuration which can be said to induce a bias in the data records. Furthermore, the results from chapter four of inducing variation based on both buoy as well as altimeter errors onto the original buoy time series has a minimal impact on the overall annual mean and 90th percentile trends. In regards to question two from chapter one, we show in chapter four that the uncertainty induced on buoy mean and 90th percentile trends is on the order of millimeters per year, while the trends themselves are on the order of centimeters per year. In regards to question three from chapter one, we show that the uncertainty in trends increases at the 99th percentile, showing a distinct difference with the uncertainty at the mean and the 90th percentile. With this in mind, buoy records should be regarded as a data source from which annual mean and 90th percentile trends can

Table 5.1 Buoy WMO46005 is deployed off of the coast of the state of Washington and buoy WMO46002 is deployed off of the coast of the state of Oregon, both along the USA west coast. Trends are estimated for annual averages and 50 year increases in wave height are calculated from these trends (assuming a continuous linear rate).

46005 Trend	*46005 50-yr*	*46002 Trend*	*46002 50-yr*	*Study*
2.7 $cmyr^{-1}$	135 cm	1.3 $cmyr^{-1}$	65 cm	(Allan and Komar 2000)
2.1 $cmyr^{-1}$	105 cm	1.9 $cmyr^{-1}$	95 cm	(Gower 2002)
2.0 $cmyr^{-1}$	100 cm	2.0 $cmyr^{-1}$	100 cm	(Menéndez et al. 2009)
1.5 $cmyr^{-1}$	75 cm	1.0 $cmyr^{-1}$	50 cm	(Ruggiero et al. 2010)
0.3 $cmyr^{-1}$	15 cm	-0.2 $cmyr^{-1}$	-10 cm	(Gemmrich et al. 2011)
-0.2 $cmyr^{-1}$	-10 cm	-0.3 $cmyr^{-1}$	-15 cm	M.S. Thesis Leyva (Stopa)

be derived with confidence.

5.3 Outlook

In this study we use synthetic time series to estimate the uncertainty associated with buoy trends based on yearly statistics. Using the same synthetic time series technique it is also possible to estimate the uncertainty of the seasonal statistics or monthly statistics. Also, the synthetic time series could also be created by propagating residuals only within months rather than propagating all residuals from time series throughout entire time series. Similarly, residuals could be propagated within specific buoy configurations.

Another method that can be used to understand the uncertainty of significant wave height records is by first finding the uncertainty range of individual wave height measurements for buoy. The NDBC network reports a tolerance range of ± 0.2 m for most payloads. Mathematically, this tolerance range can be used to derive the tolerance range for significant

wave height and for trends as well.

Also, this study can be expanded to include more buoys. While the technique to create synthetic time series used altimeter data starting at 1985, during that initial period there was only one satellite in orbit followed by a two year period with no satellites in orbit. There may be advantages to only considering data after 1993, because this is when there are multiple satellites in orbit which can be used to cross-validate their measurements (Young et al. 2017). In a few years, with data available for the year 2023, this will give a data record of 30 years (starting from 1993) which can be analyzed with greater confidence due to multiple satellites being in orbit throughout this time period. While longer data records would be preferred in order to reduce the impacts of inter-annual variability on the time series, a trade-off needs to be made in terms of length of data record vs. quality of data record. By limiting the data records in this study to 1985 and beyond, the quality of the data record is significantly improved. By limiting the data records to 1993 and beyond for future studies, this will only further improve the quality of the data records, while only excluding eight years from the overall time series.

Appendix A

Altimeter Dependence on Individual Buoys

Table A.1 Percentage of Buoy Data Used in Altimeter Calibration

Altimer	Time Period	41001	41002	41040	41041	41043	41046	41047	42001	42002	42003	42039	44004	44008	44011	46001	46002	46005	46006	46035	51001	51003	51004	51028
Geosat	31 Mar 1985–30 Dec 1989	1.5%	0.0%	0.0%	0.0%	0.0%	0.0%	0.0%	0.9%	1.7%	0.6%	0.0%	0.0%	0.0%	5.1%	12.2%	1.3%	6.9%	6.6%	6.0%	4.9%	1.7%	0.0%	0.0%
ERS-1	1 Aug 1991–2 Jun 1996	3.2%	0.0%	0.0%	0.0%	0.0%	0.0%	0.0%	1.0%	0.1%	1.6%	0.2%	6.6%	0.4%	2.5%	8.7%	0.0%	5.1%	0.0%	0.0%	0.0%	4.4%	0.0%	0.0%
TOPEX	25 Sep 1992–25 Apr 1997	10.1%	0.0%	0.0%	0.0%	0.0%	0.0%	0.0%	0.0%	5.5%	3.6%	1.7%	5.0%	0.0%	0.0%	10.6%	0.0%	4.9%	0.0%	9.8%	0.0%	5.7%	0.0%	0.0%
TOPEX	30 Jan 1999–8 Oct 2005	4.1%	3.0%	0.1%	0.1%	0.0%	0.0%	0.0%	1.5%	3.5%	3.3%	1.8%	3.1%	3.0%	2.4%	8.1%	2.2%	3.6%	3.5%	4.4%	1.5%	3.9%	2.0%	3.7%
ERS-2	29 Apr 1995–11 May 2009	4.0%	3.5%	0.0%	0.0%	0.5%	0.5%	0.4%	3.1%	3.5%	2.6%	2.6%	3.6%	4.6%	5.3%	7.7%	6.0%	7.1%	4.1%	4.1%	4.4%	2.4%	2.5%	1.5%
GFO	7 Jan 2000–7 Sep 2008	2.4%	4.3%	0.8%	1.3%	0.7%	0.2%	0.3%	2.4%	1.3%	2.3%	0.0%	2.7%	4.9%	1.9%	8.0%	3.5%	5.0%	3.2%	4.8%	5.6%	2.4%	3.0%	2.3%
Jason-1	15 Jan 2002–3 Mar 2012	3.9%	0.0%	1.8%	1.3%	1.5%	2.4%	1.3%	0.6%	2.0%	2.4%	2.2%	2.1%	0.9%	0.8%	7.7%	1.1%	3.1%	2.0%	6.6%	0.0%	3.7%	0.0%	2.0%
Envisat	14 May 2002–1 Aug 2004	4.4%	4.7%	0.0%	0.0%	0.0%	0.0%	0.0%	2.7%	4.5%	2.4%	3.2%	3.9%	3.8%	5.3%	6.8%	3.2%	7.4%	3.5%	7.3%	5.7%	2.7%	2.7%	2.7%
Envisat	1 Aug 2004–8 Apr 2012	1.7%	1.0%	3.1%	2.1%	1.5%	1.7%	1.4%	1.7%	1.4%	1.4%	1.6%	1.2%	3.2%	2.4%	4.2%	2.4%	2.2%	2.0%	3.6%	3.0%	2.1%	1.3%	0.9%
Jason-2	22 Jun 2008–10 May 2012	2.9%	0.0%	0.0%	2.7%	5.5%	0.0%	1.8%	0.0%	1.4%	1.4%	1.3%	0.0%	0.0%	0.0%	5.4%	0.0%	1.2%	0.0%	3.7%	0.0%	2.7%	0.0%	0.0%
CryoSat	14 Jul 2010–1 Apr 2015	2.2%	2.4%	3.4%	3.8%	3.7%	3.8%	3.2%	1.5%	1.5%	2.2%	1.8%	0.0%	2.3%	1.0%	6.6%	4.2%	2.2%	2.7%	1.4%	0.0%	3.8%	3.0%	0.0%

Appendix B

Hull, Payload, and Processor ID Numbering System

NDBC/MEDS HULLS assigns hull id numbers based on metadata, organizes into hulls types and specific serial numbers.

Hull Id Number Key (hln), numbers in thousandth places indicate hull size:

23000=2.3(m); 30000=3(m); 60000=6(m);100000=10(m); 120000=12(m);

Numbers in hundredth place indicates other variations

1='C'(MEDS); 2='M'; 6='V'(Foam Hull)

Numbers in the tenth place and ones place indicate hull serial number

(ie. 6N05=05, 12D03=03)

NDBC/MEDS PAYLOADS assigns payload id numbers based on metadata, organizes into payload types and specific wmo serial numbers.

Payload Id Number Key (pln), numbers in the ten and hundred thousandth places indicates payload type:

NDBC

10000='SCOOP'(1);

20000='AMPS'(2);

30000='ARES'(3);

40000='MARS'(4);

50000=’VEEP’(5);

60000=’DACT’(6);

70000=’GSBP’(7);

80000=’UDACS(A)’(8);

90000=’MVXII’(9);

100000=’UDACS’(10);

110000=’DACS’(11);

120000=’PEB’(12);

130000=’EEP’(13);

MEDS

140000=’WM’(14);

150000=’ZE’(15);

160000=’*’(16);

Numbers in thousandth, hundredth and tenth place indicates serial number

(ie. ’WM026’=026)

Numbers in the ones place indicates other slight variation

’/’(1);

’Mars’ lower case (5);

’O’vs’0’(8);

NDBC PROCESSORS assigns processor id numbers based on metadata organizes into payload types and specific wmo serial numbers

Processor Id Number Key (prn) Numbers in the ten and hundred thousandth places indicates payload type:

NDBC

15000=’DDWM’(1);

25000='DWPM'(2);

35000='WPM'(3);

65000='WA'(6);

95000='WDA'(9);

125000='WSA'(12);

135000='EEP'(13);

DWWRHULLS assigns payload id numbers based on metadata organizes into payload types and specific cdip serial numbers

Hull Id Number Key (hln) numbers in hundred thousandth place indicates waverider hull model:

100000='FL';

200000='Mark 2';

300000='Mark 3';

400000='Mark 4'

(*this number is assigned for cdip buoys by checking if tophat)

Serial number (payload) starts with a letter

Numbers in ten thousandth place indicates Directional or Non-Directiinal:

0='Non-Directional';

2='Directional';

(*this numer is assigned for imos buoys in metadataimos function)

Numbers in thousandth, hundredth, and tenth places indicates cdip hull serial number (all cdip hull serial numbers start with '30' so this is not included):

(ie. 30883=883, 30265=265)

Number in the ones place indicates other slight variation

1='a';

2='b';

3='c';

DWWRPAYLOADS tophat serial number only for cdip

Payload Id Number Key (pln) numbers in hundred thousandth place indicates if serial number has more 5 numbers or if there are letters included as well:

0='Less than 6 numbers';

1='B1';

2='B1'and 'G';

3='B1' and 'CG';

4='NA';

Numbers in thousandth, hundredth, tenth and ones place indicate cdip serial number (dashes not included):

ie. NA-388=400388, B157126=157126

Appendix C

Procedure Used for RHtestsV4

The following outlines the procedure we used to execute RHtestsV4 in an unbiased, objective manner. The procedure is adapted from guidelines in "RHtestsV4 User Manual" (Wang and Feng 2013).

a) Choose reference series to compare base series to. Analysis is less reliable without a reference series, particularly because the seasonality of wave data makes the time series more variable making step changes more difficult to identify.

b) Analyze the reference series alone (treating it as a base series with no reference series). If no change points are identified, the reference series can be said to be homogenous. If change points are identified the series may not be suitable to be used as a reference series, as change points identified may be due to the inhomogeneity of the reference series rather than the base series.

c) Co-locate between buoy, and hindcast or altimeter to the nearest hour. When a time series has multiple observations in an hour the observations will be averaged.

d) From the new time series create a monthly average base time series and a monthly average reference time series. The minimum number of days with observations per month is chosen to be four days of observations. If a month only has a few observations and the observations are very different between the base series and the reference series this would put a lot of weight on those few observations. Only creating monthly averages for months with at least 4 different days of observations will reduce the impact of outliers impacting the

data.

e) Create text files for the monthly base series and monthly reference series in the format specified by the RHtestsV4 user manual.

f) To run RHtest using RStudio, instructions are in the RHtestsV4 user manual, and are also outlined below.

1) Open RStudio

2) Within RStudio open RHtestsV4_20130719.r

3) Click "Source"

4) In command prompt type "StartGUI()" and click enter

5) Click "I Agree" on GUI pop-up

6) Click "Change Pars" and change "Missing Value Code" to "NaN"

7) Leave other values as defaults:

7.1) Confidence Level: 0.95

7.2) Integer Adjustment: 10000 (corresponds to last segment to adjust data)

7.3) Mq: 12 (number of points for which empirical pdf to be estimated)

7.4) Ny4a: 0 (corresponds to using whole segment of data to estimate pdf)

8) Click "OK" to save parameters.

9) To test homogeneity of base series click "FindU".

10) Click "Change" and choose monthly averaged base series.

11) If no change points are identified the base series can be said to be homogenous

12) If change points are identified click "FindUD".

13) Review list of identified changed points. Remove all type-0 change points with no reliable metadata within +/- 3 months of change.

14) Click "Step Size" to reassess change points based on current list.

15) Remove any change points that say "No".

16) Repeat steps "14" and "15" until there are no more change points to remove. This is the final list of changepoints.

17) To test homogeneity of reference series click "FindU".

18) Click "Change" and choose monthly averaged reference series.

19) If no change points are identified the reference series can be said to be homogenous, if change points are identified reference series is not for suitable for analysis with base series.

20) To analyze base series with a homogenous reference series click "FindU.wRef"

21) For Input Base Data filename click "Change" and select buoy monthly series.

22) For Ref Base Data filename click "Change" and select reference monthly series.

23) If no change points are identified the buoy series can be said to be homogenous relative to the homogenous reference series.

24) If change points are identified click "FindUD.wRef" to identify change points that are significant only if accompanied by reliable metadata (type-0 change points)

25) Review list of identified change points. Remove all type-0 change points with no reliable metadata within +/- 3 months of change.

26) Click "Step Size" to reassess change points based on current list.

27) Remove any change points that say "No".

28) Review list of identified change points. Change all type-0 change points with reliable metadata to metadata date.

29) Repeat steps "26" and "27" until there are no more change points to remove. This is the final list of changepoints.

Appendix D

RHtestsV4 and Zonation Results

Results from RHtestsV4 and zonation for buoys WMO41001, WMO42003, WMO46001, and WMO46005, are on the following pages.

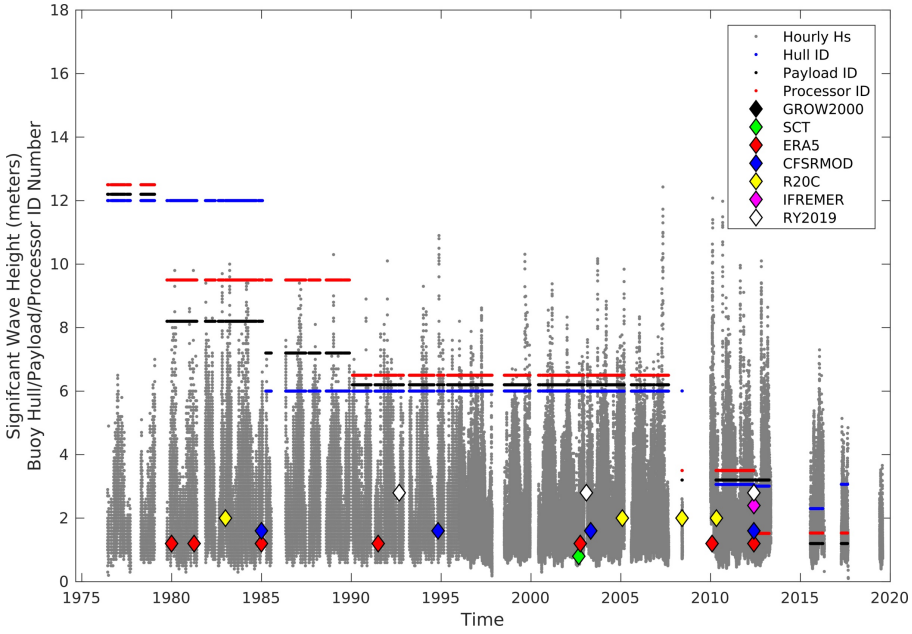

Figure D.1 Change points identified with RHtestsV4 for buoy WMO41001

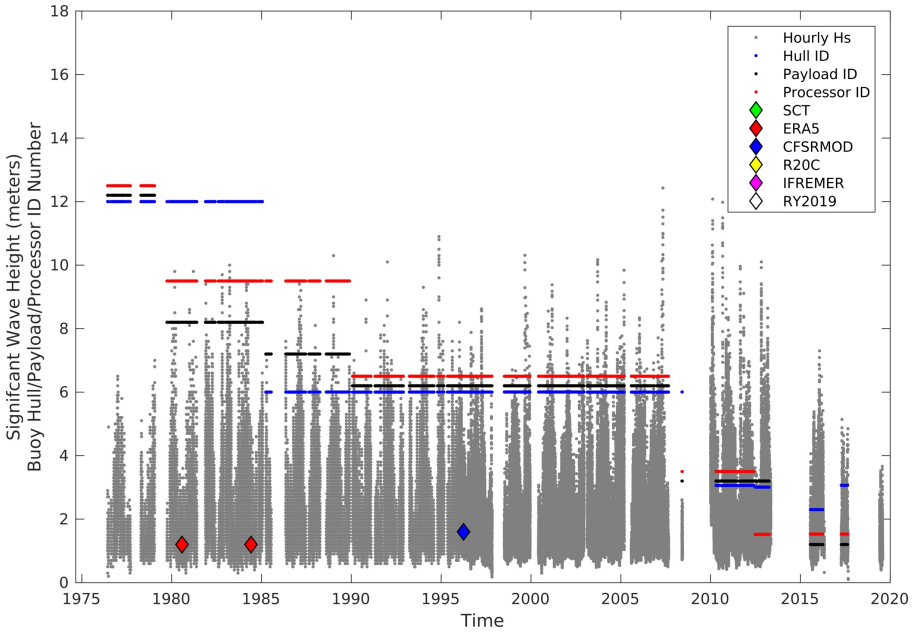

Figure D.2 Change points identified with zonation for buoy WMO41001

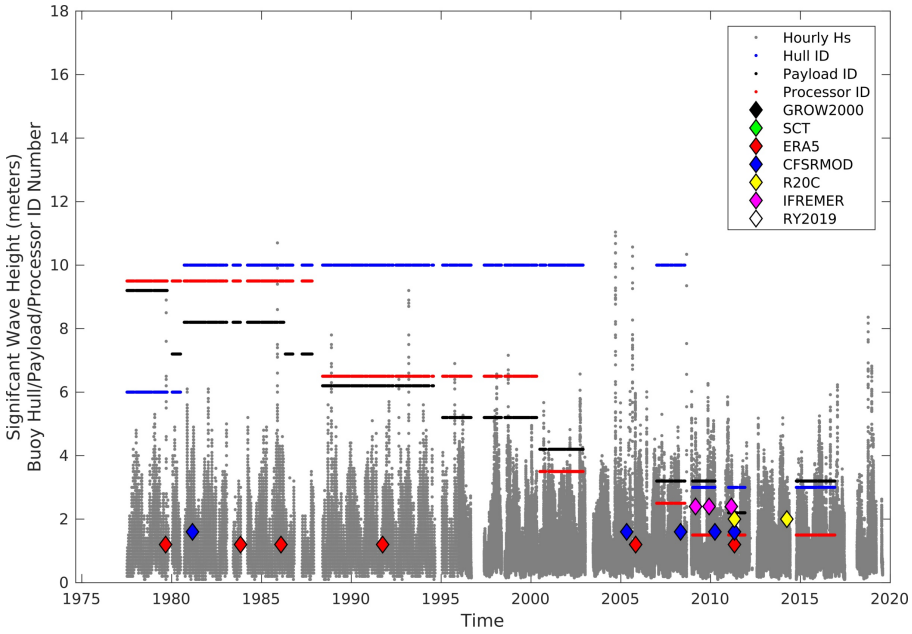

Figure D.3 Change points identified with RHtestsV4 for buoy WMO42003

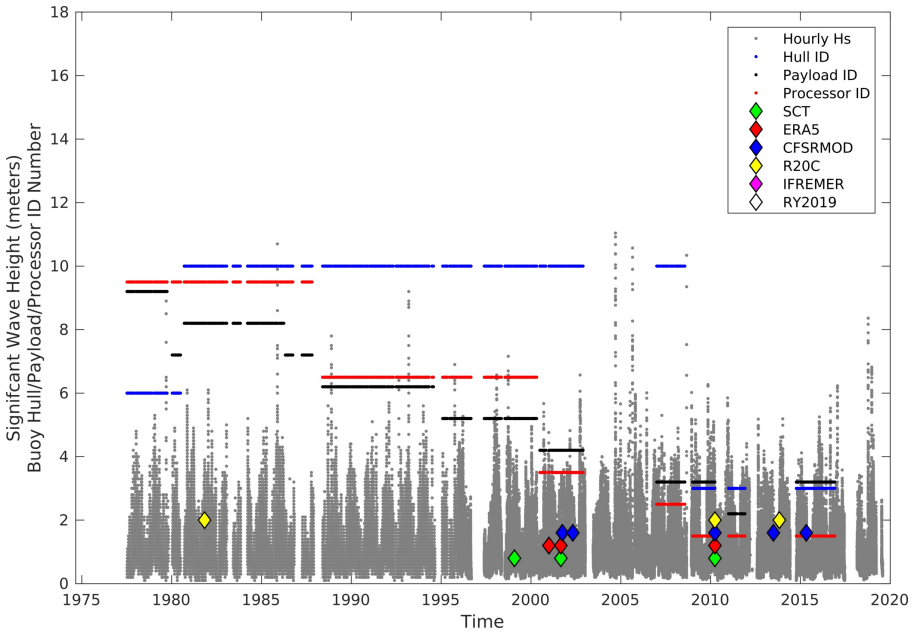

Figure D.4 Change points identified with zonation for buoy WMO42003

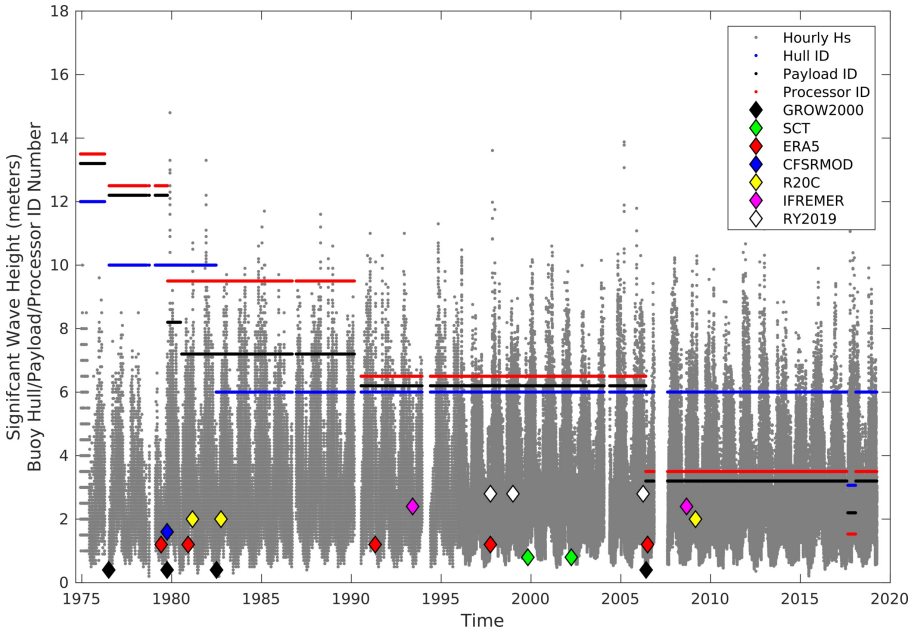

Figure D.5 Change points identified with RHtestsV4 for buoy WMO46001

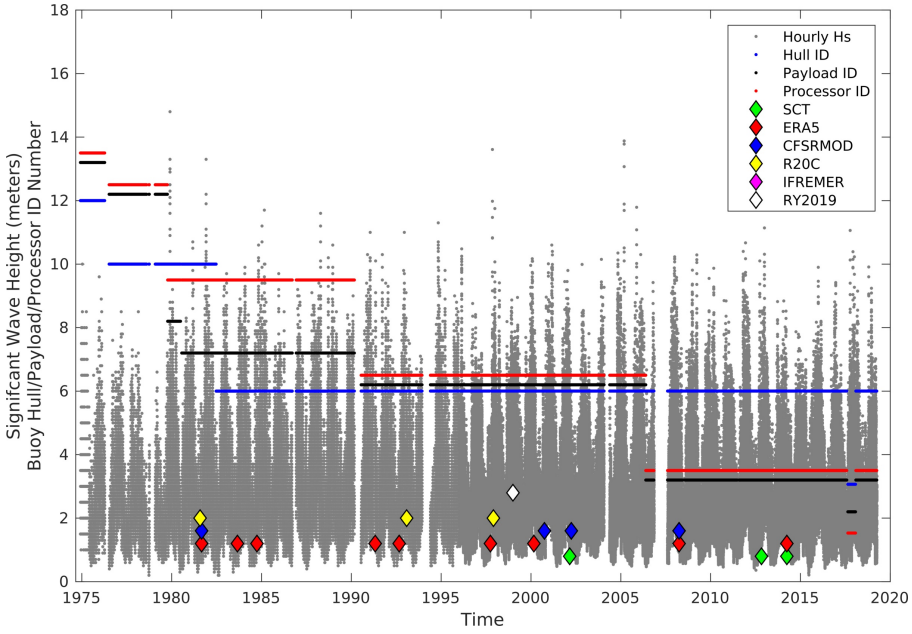

Figure D.6 Change points identified with zonation for buoy WMO46001

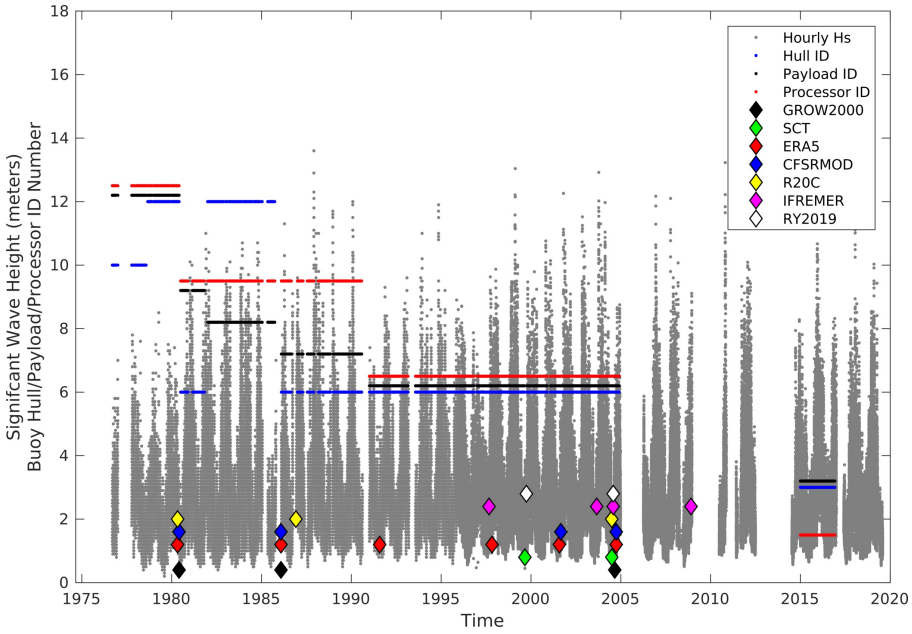

Figure D.7 Change points identified with RHtestsV4 for buoy WMO46005

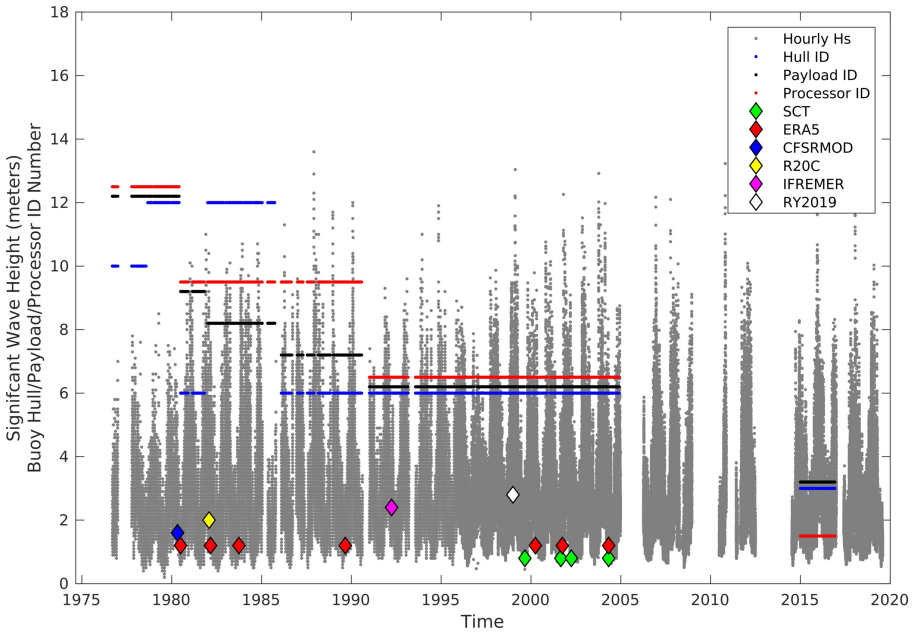

Figure D.8 Change points identified with zonation for buoy WMO46005

Appendix E

Images of Different Types of Buoys

Figure E.1 NDBC 12-meter discus buoy (NDBC 2020b)

Figure E.2 NDBC 10-meter discus buoy (NDBC 2020a)

Figure E.3 NDBC 6-meter discus buoy (NDBC 2020d)

Figure E.4 NDBC 3-meter discus buoy (NDBC 2020c)

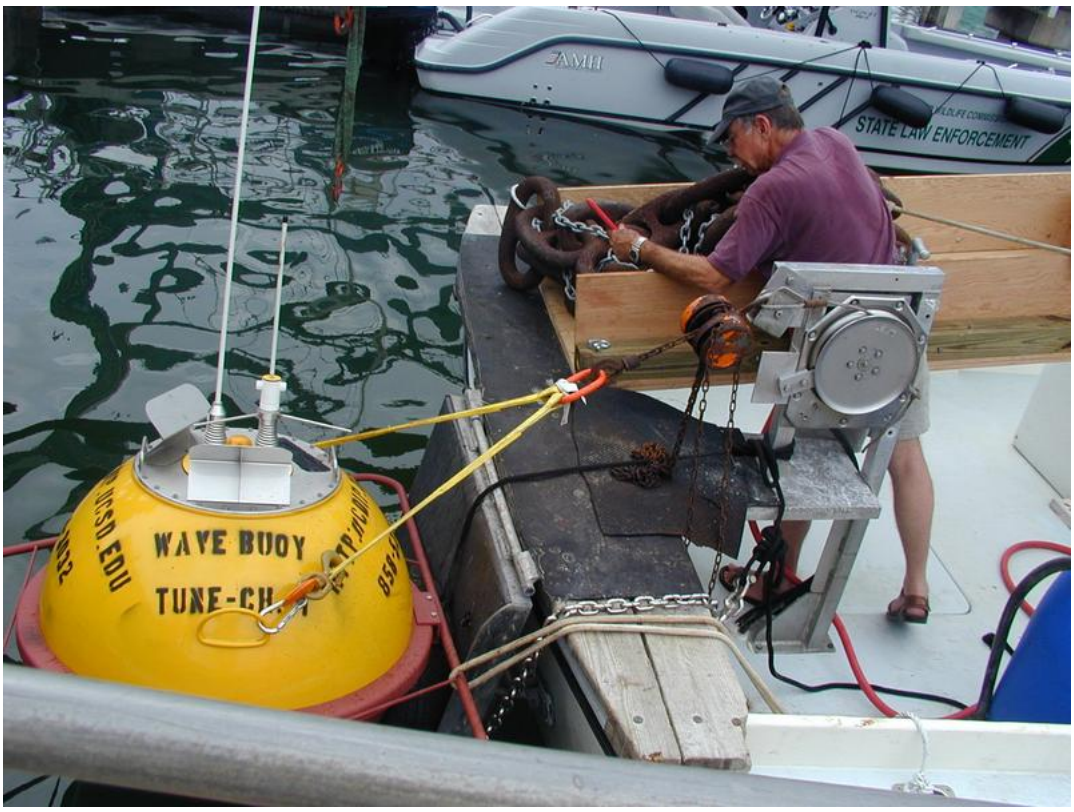

Figure E.5 CDIP Datawell Waverider (CDIP 2020)

Bibliography

Aarnes, Ole Johan, Saleh Abdalla, Jean-Raymond Bidlot, and Øyvind Breivik. 2015. "Marine Wind and Wave Height Trends at Different ERA-Interim Forecast Ranges" [in en]. *Journal of Climate* 28, no. 2 (January): 819–837. ISSN: 0894-8755, 1520-0442, accessed September 2, 2019. doi:10.1175/JCLI-D-14-00470.1. http://journals.ametsoc.org/doi/10.1175/JCLI-D-14-00470.1.

Allan, Jonathan, and Paul Komar. 2000. "Are ocean wave heights increasing in the eastern North Pacific?" [In en]. *Eos, Transactions American Geophysical Union* 81 (47): 561–567. ISSN: 2324-9250, accessed September 2, 2019. doi:10.1029/EO081i047p00561-01. http://agupubs.onlinelibrary.wiley.com/doi/abs/10.1029/EO081i047p00561-01.

Ardhuin, Fabrice, Justin E. Stopa, Bertrand Chapron, Fabrice Collard, Romain Husson, Robert E. Jensen, Johnny Johannessen, Alexis Mouche, Marcello Passaro, Graham D. Quartly, Val Swail, and Ian Young. 2019. "Observing Sea States" [in English]. *Frontiers in Marine Science* 6. ISSN: 2296-7745, accessed March 1, 2020. doi:10.3389/fmars.2019.00124. https://www.frontiersin.org/articles/10.3389/fmars.2019.00124/full.

Bentamy, Abderrahim, Semyon A. Grodsky, Anis Elyouncha, Bertrand Chapron, and Fabien Desbiolles. 2017. "Homogenization of scatterometer wind retrievals: HOMOGENEOUS SCATTEROMETER SURFACE WIND VECTOR OBSERVATIONS" [in en]. *International Journal of Climatology* 37, no. 2 (February): 870–889. ISSN: 08998418, accessed July 23, 2020. doi:10.1002/joc.4746. http://doi.wiley.com/10.1002/joc.4746.

Brigham, E. Oran. 1988. *The fast Fourier transform and its applications* [in en]. Prentice-Hall signal processing series. Englewood Cliffs, N.J: Prentice Hall. ISBN: 978-0-13-307505-2.

Cai, Wenju, Simon Borlace, Matthieu Lengaigne, Peter van Rensch, Mat Collins, Gabriel Vecchi, Axel Timmermann, Agus Santoso, Michael J. McPhaden, Lixin Wu, Matthew H. England, Guojian Wang, Eric Guilyardi, and Fei-Fei Jin. 2014. "Increasing frequency of extreme El Niño events due to greenhouse warming" [in en]. *Nature Climate Change* 4, no. 2 (February): 111–116. ISSN: 1758-6798, accessed March 1, 2020. doi:10.1038/nclimate2100. https://www-nature-com.eres.library.manoa.hawaii.edu/articles/nclimate2100.

CDIP. 2020. *hustler2.jpg (JPEG Image, 800 600 pixels) - Scaled (81%).* Accessed March 2. http://cdip.ucsd.edu/themes/media/images/document_images/deploy_docs/hustler2.jpg.

Chawla, Arun, Deanna M. Spindler, and Hendrik L. Tolman. 2013. "Validation of a thirty year wave hindcast using the Climate Forecast System Reanalysis winds" [in en]. *Ocean*

Modelling, Ocean Surface Waves, 70 (October): 189–206. ISSN: 1463-5003, accessed July 21, 2020. doi:10.1016/j.ocemod.2012.07.005. http://www.sciencedirect.com/science/article/pii/S1463500312001047.

Compo, G. P., J. S. Whitaker, P. D. Sardeshmukh, N. Matsui, R. J. Allan, X. Yin, B. E. Gleason, R. S. Vose, G. Rutledge, P. Bessemoulin, S. Brönnimann, M. Brunet, R. I. Crouthamel, A. N. Grant, P. Y. Groisman, P. D. Jones, M. C. Kruk, A. C. Kruger, G. J. Marshall, M. Maugeri, H. Y. Mok, Ø Nordli, T. F. Ross, R. M. Trigo, X. L. Wang, S. D. Woodruff, and S. J. Worley. 2011. "The Twentieth Century Reanalysis Project" [in en]. _eprint: https://onlinelibrary.wiley.com/doi/pdf/10.1002/qj.776, *Quarterly Journal of the Royal Meteorological Society* 137 (654): 1–28. ISSN: 1477-870X, accessed July 23, 2020. doi:10.1002/qj.776. http://rmets.onlinelibrary.wiley.com/doi/abs/10.1002/qj.776.

Datawell. 2020. *Datawell > Buoys,* January. Accessed May 20, 2020. http://www.datawell.nl/products/buoys.aspx.

Fan, Yalin, Shian-Jiann Lin, Stephen M. Griffies, and Mark A. Hemer. 2014. "Simulated Global Swell and Wind-Sea Climate and Their Responses to Anthropogenic Climate Change at the End of the Twenty-First Century." *Journal of Climate* 27, no. 10 (January): 3516–3536. ISSN: 0894-8755, accessed March 1, 2020. doi:10.1175/JCLI-D-13-00198.1. https://journals-ametsoc-org.eres.library.manoa.hawaii.edu/doi/full/10.1175/JCLI-D-13-00198.1.

Gemmrich, Johannes, Bridget Thomas, and Richard Bouchard. 2011. "Observational changes and trends in northeast Pacific wave records: NE PACIFIC WAVE TRENDS" [in en]. *Geophysical Research Letters* 38, no. 22 (November): n/a–n/a. ISSN: 00948276, accessed September 2, 2019. doi:10.1029/2011GL049518. http://doi.wiley.com/10.1029/2011GL049518.

Gower, J. F. R. 2002. "Temperature, Wind and Wave Climatologies, and Trends from Marine Meteorological Buoys in the Northeast Pacific." *Journal of Climate* 15, no. 24 (December): 3709–3718. ISSN: 0894-8755, accessed March 1, 2020. doi:10.1175/1520-0442(2002)015<3709:TWAWCA>2.0.CO;2. https://journals-ametsoc-org.eres.library.manoa.hawaii.edu/doi/full/10.1175/1520-0442%282002%29015%3C3709%3ATWAWCA%3E2.0.CO%3B2.

Gulev, Sergey K., and Vika Grigorieva. 2006. "Variability of the Winter Wind Waves and Swell in the North Atlantic and North Pacific as Revealed by the Voluntary Observing Ship Data" [in en]. Publisher: American Meteorological Society, *Journal of Climate* 19, no. 21 (November): 5667–5685. ISSN: 0894-8755, accessed July 3, 2020. doi:10.1175/JCLI3936.1. https://journals-ametsoc-org.eres.library.manoa.hawaii.edu/jcli/article/19/21/5667/31330/Variability-of-the-Winter-Wind-Waves-and-Swell-in.

Hoeke, Ron K., Kathleen L. McInnes, Jens C. Kruger, Rebecca J. McNaught, John R. Hunter, and Scott G. Smithers. 2013. "Widespread inundation of Pacific islands triggered by distant-source wind-waves" [in en]. *Global and Planetary Change* 108 (September): 128–138. ISSN: 09218181, accessed September 2, 2019. doi:10.1016/j.gloplacha.2013.06.006. https://linkinghub.elsevier.com/retrieve/pii/S0921818113001483.

Izaguirre, Cristina, Fernando J. Méndez, Melisa Menéndez, and Inigo J. Losada. 2011. "Global extreme wave height variability based on satellite data" [in en]. *Geophysical Research Letters* 38 (10). ISSN: 1944-8007, accessed July 29, 2020. doi:10.1029/2011GL047302. http://agupubs.onlinelibrary.wiley.com/doi/abs/10.1029/2011GL047302.

Koch, Alexander, Chris Brierley, Mark M. Maslin, and Simon L. Lewis. 2019. "Earth system impacts of the European arrival and Great Dying in the Americas after 1492" [in en]. *Quaternary Science Reviews* 207 (March): 13–36. ISSN: 02773791, accessed July 21, 2020. doi:10.1016/j.quascirev.2018.12.004. https://linkinghub.elsevier.com/retrieve/pii/S0277379118307261.

Lefèvre, Jean-Michel. 2009. "High swell warnings in the Caribbean islands during march 2008" [in en]. *Natural Hazards* 49, no. 2 (May): 361–370. ISSN: 0921-030X, 1573-0840, accessed September 2, 2019. doi:10.1007/s11069-008-9323-6. http://link.springer.com/10.1007/s11069-008-9323-6.

Longuet-Higgins, M. S. 1957. "The Statistical Analysis of a Random, Moving Surface." Publisher: The Royal Society, *Philosophical Transactions of the Royal Society of London. Series A, Mathematical and Physical Sciences* 249 (966): 321–387. ISSN: 0080-4614, accessed June 23, 2020. https://www.jstor.org/stable/91668.

———. 1984. "Statistical Properties of Wave Groups in a Random Sea State." Publisher: The Royal Society, *Philosophical Transactions of the Royal Society of London. Series A, Mathematical and Physical Sciences* 312 (1521): 219–250. ISSN: 0080-4614, accessed July 20, 2020. https://www.jstor.org/stable/37397.

Longuet-Higgins, Michael S. 1980. "On the distribution of the heights of sea waves: Some effects of nonlinearity and finite band width" [in en]. *Journal of Geophysical Research: Oceans* 85 (C3): 1519–1523. ISSN: 2156-2202, accessed June 23, 2020. doi:10.1029/JC085iC03p01519. http://agupubs.onlinelibrary.wiley.com/doi/abs/10.1029/JC085iC03p01519.

Menéndez, Melisa, Fernando J. Méndez, Cristina Izaguirre, Alberto Luceño, and Inigo J. Losada. 2009. "The influence of seasonality on estimating return values of significant wave height" [in en]. *Coastal Engineering* 56, no. 3 (March): 211–219. ISSN: 03783839, accessed June 22, 2020. doi:10.1016/j.coastaleng.2008.07.004. https://linkinghub.elsevier.com/retrieve/pii/S0378383908001269.

Menéndez, Melisa, Fernando J. Méndez, Inigo J. Losada, and Nicholas E. Graham. 2008. "Variability of extreme wave heights in the northeast Pacific Ocean based on buoy measurements" [in en]. *Geophysical Research Letters* 35 (22). ISSN: 1944-8007, accessed March 1, 2020. doi:10.1029/2008GL035394. http://agupubs.onlinelibrary.wiley.com/doi/abs/10.1029/2008GL035394.

NDBC. 2020a. *10m.jpg (JPEG Image, 354 × 480 pixels)*. Accessed March 2. https://www.ndbc.noaa.gov/images/buoys/10m.jpg.

———. 2020b. *12m.* Accessed March 2. https://www.ndbc.noaa.gov/images/buoys/12m.jpg.

———. 2020c. *3moly.jpg (JPEG Image, 404 × 480 pixels)*. Accessed March 2. https://www.ndbc.noaa.gov/images/buoys/3moly.jpg.

———. 2020d. *6m.jpg (JPEG Image, 368 × 480 pixels)*. Accessed March 2. https://www.ndbc.noaa.gov/images/buoys/6m.jpg.

NDBC, NOAA. 2009. *National Data Buoy Center* [in EN-US], August. Accessed June 24, 2020. https://www.ndbc.noaa.gov/qc.shtml.

———. 2012. *National Data Buoy Center* [in EN-US], June. Accessed June 24, 2020. https://www.ndbc.noaa.gov/hull.shtml.

———. 2017. *National Data Buoy Center* [in EN-US], February. Accessed June 24, 2020. https://www.ndbc.noaa.gov/rsa.shtml.

———. 2018. *National Data Buoy Center* [in EN-US], March. Accessed June 24, 2020. https://www.ndbc.noaa.gov/wave.shtml.

Neukom, Raphael, Nathan Steiger, Juan José Gómez-Navarro, Jianghao Wang, and Johannes P. Werner. 2019. "No evidence for globally coherent warm and cold periods over the preindustrial Common Era" [in en]. Number: 7766 Publisher: Nature Publishing Group, *Nature* 571, no. 7766 (July): 550–554. ISSN: 1476-4687, accessed July 21, 2020. doi:10.1038/s41586-019-1401-2. http://www.nature.com/articles/s41586-019-1401-2.

NOAA. 2014. *FAQ* [in en-US]. Library Catalog: noaabuoydata.com, April. Accessed May 20, 2020. http://noaabuoydata.com/faq/.

Queensland Government. 2019. *Glossary | Wave monitoring* [in en]. Last Modified: 2019-02-26 Library Catalog: www.qld.gov.au Publisher: corporateName=The State of Queensland; jurisdiction=Queensland, February. Accessed June 24, 2020. https://www.qld.gov.au/environment/coasts-waterways/beach/monitoring/waves-glossary.

Reguero, B.G., M. Menéndez, F.J. Méndez, R. Mínguez, and I.J. Losada. 2012. "A Global Ocean Wave (GOW) calibrated reanalysis from 1948 onwards" [in en]. *Coastal Engineering* 65 (July): 38–55. ISSN: 03783839, accessed September 2, 2019. doi:10.1016/j.coastaleng.2012.03.003. https://linkinghub.elsevier.com/retrieve/pii/S0378383912000452.

Ribal, Agustinus, and Ian R. Young. 2019. "33 years of globally calibrated wave height and wind speed data based on altimeter observations" [in en]. *Scientific Data* 6, no. 1 (December): 77. ISSN: 2052-4463, accessed August 5, 2020. doi:10.1038/s41597-019-0083-9. http://www.nature.com/articles/s41597-019-0083-9.

Roemmich, Dean, John Church, John Gilson, Didier Monselesan, Philip Sutton, and Susan Wijffels. 2015. "Unabated planetary warming and its ocean structure since 2006" [in en]. *Nature Climate Change* 5, no. 3 (March): 240–245. ISSN: 1758-6798, accessed March 1, 2020. doi:10.1038/nclimate2513. https://www-nature-com.eres.library.manoa.hawaii.edu/articles/nclimate2513.

Ruggiero, Peter, Paul D. Komar, and Jonathan C. Allan. 2010. "Increasing wave heights and extreme value projections: The wave climate of the U.S. Pacific Northwest" [in en]. *Coastal Engineering* 57, no. 5 (May): 539–552. ISSN: 0378-3839, accessed March 1, 2020. doi:10.1016/j.coastaleng.2009.12.005. http://www.sciencedirect.com/science/article/pii/S0378383909002142.

Saha, Suranjana, Shrinivas Moorthi, Xingren Wu, Jiande Wang, Sudhir Nadiga, Patrick Tripp, David Behringer, Yu-Tai Hou, Hui-ya Chuang, Mark Iredell, Michael Ek, Jesse Meng, Rongqian Yang, Malaquías Peña Mendez, Huug van den Dool, Qin Zhang, Wanqiu Wang, Mingyue Chen, and Emily Becker. 2014. "The NCEP Climate Forecast System Version 2" [in en]. Publisher: American Meteorological Society, *Journal of Climate* 27, no. 6 (March): 2185–2208. ISSN: 0894-8755, accessed July 20, 2020. doi:10.1175/JCLI-D-12-00823.1. https://journals-ametsoc-org.eres.library.manoa.hawaii.edu/jcli/article/27/6/2185/34842/The-NCEP-Climate-Forecast-System-Version-2.

Shimura, Tomoya, Nobuhito Mori, and Mark A. Hemer. 2016. "Variability and future decreases in winter wave heights in the Western North Pacific" [in en]. *Geophysical Research Letters* 43, no. 6 (March): 2716–2722. ISSN: 0094-8276, 1944-8007, accessed September 2, 2019. doi:10.1002/2016GL067924. https://onlinelibrary.wiley.com/doi/abs/10.1002/2016GL067924.

Steele, K. E., D. W. Wang, M. D. Earle, E. D. Michelena, and R. J. Dagnall. 1998. "Buoy pitch and roll computed using three angular rate sensors" [in en]. *Coastal Engineering* 35, no. 1 (October): 123–139. ISSN: 0378-3839, accessed July 20, 2020. doi:10.1016/S0378-3839(98)00025-8. http://www.sciencedirect.com/science/article/pii/S0378383998000258.

Steele, K.E., and M.D. Earle. 1991. "Directional ocean wave spectra using buoy azimuth, pitch, and roll derived from magnetic field components." *IEEE Journal of Oceanic*

Engineering 16, no. 4 (October): 427–433. ISSN: 03649059, accessed June 23, 2020. doi:10.1109/48.90909. http://ieeexplore.ieee.org/document/90909/.

Stopa, Justin E. 2018. "Wind forcing calibration and wave hindcast comparison using multiple reanalysis and merged satellite wind datasets" [in en]. *Ocean Modelling* 127 (July): 55–69. ISSN: 14635003, accessed May 22, 2020. doi:10.1016/j.ocemod.2018.04.008. https://linkinghub.elsevier.com/retrieve/pii/S1463500318301458.

Stopa, Justin E., Fabrice Ardhuin, Eleonore Stutzmann, and Thomas Lecocq. 2019. "Sea State Trends and Variability: Consistency Between Models, Altimeters, Buoys, and Seismic Data (1979–2016)" [in en]. *Journal of Geophysical Research: Oceans* 124 (6): 3923–3940. ISSN: 2169-9291, accessed July 21, 2020. doi:10.1029/2018JC014607. http://agupubs.onlinelibrary.wiley.com/doi/abs/10.1029/2018JC014607.

Swan, A. R. H., and M. Sandilands. 1995. *Introduction to Geological Data Analysis.* Blackwell Science.

Thomas, B., and Val Swail. 2009. "Long term wave measurements and trend at Canadian coastal locations." In *Eleventh International Workshop on Wave Hindcasting and Forecasting and Second Coastal Hazard Symposium.* Halifax, Canada, October.

Timmermans, B. W., C. P. Gommenginger, G. Dodet, and J.-R. Bidlot. 2020. "Global Wave Height Trends and Variability from New Multimission Satellite Altimeter Products, Reanalyses, and Wave Buoys" [in en]. *Geophysical Research Letters* 47 (9): e2019GL086880. ISSN: 1944-8007, accessed July 23, 2020. doi:10.1029/2019GL086880. http://agupubs.onlinelibrary.wiley.com/doi/abs/10.1029/2019GL086880.

Wan, Hui, Xiaolan L. Wang, and Val R. Swail. 2010. "Homogenization and Trend Analysis of Canadian Near-Surface Wind Speeds" [in en]. Publisher: American Meteorological Society, *Journal of Climate* 23, no. 5 (March): 1209–1225. ISSN: 0894-8755, accessed July 21, 2020. doi:10.1175/2009JCLI3200.1. https://journals-ametsoc-org.eres.library.manoa.hawaii.edu/jcli/article/23/5/1209/32841/Homogenization-and-Trend-Analysis-of-Canadian-Near.

Wang, Xiaolan L. 2003. "Comments on "Detection of Undocumented Changepoints: A Revision of the Two-Phase Regression Model"." *Journal of Climate,* no. 16 (October): 3383–3385. Accessed June 26, 2020. doi:https://doi.org/10.1175/1520-0442(2003)016<3383:CODOUC>2.0.CO;2. https://journals.ametsoc.org/jcli/article/16/20/3383/29583/Comments-on-Detection-of-Undocumented-Changepoints.

———. 2008. "Penalized Maximal F Test for Detecting Undocumented Mean Shift without Trend Change." *Journal of Atmospheric and Oceanic Technology* 25, no. 3 (March): 368–384. ISSN: 0739-0572, accessed March 1, 2020. doi:10.1175/2007JTECHA982.1.

https://journals-ametsoc-org.eres.library.manoa.hawaii.edu/doi/full/10.1175/2007JTECHA982.1.

Wang, Xiaolan L., and Yang Feng. 2009. *RHtestsV3 User Manual.*

———. 2013. *RHtestsV4 User Manual,* July. http://etccdi.pacificclimate.org/software.shtml.

Wang, Xiaolan L., Qiuzi H. Wen, and Yuehua Wu. 2007. "Penalized Maximal t Test for Detecting Undocumented Mean Change in Climate Data Series." *Journal of Applied Meteorology & Climatology* 46, no. 6 (June): 916–931. ISSN: 15588424, accessed March 1, 2020. doi:10.1175/JAM2504.1. http://eres.library.manoa.hawaii.edu/login?url=http://search.ebscohost.com/login.aspx?direct=true&db=a9h&AN=25638276&site=ehost-live.

Wentz, Frank J., Lucrezia Ricciardulli, Kyle Hilburn, and Carl Mears. 2007. "How Much More Rain Will Global Warming Bring?" Publisher: American Association for the Advancement of Science, *Science* 317 (5835): 233–235. ISSN: 0036-8075, accessed July 21, 2020. https://www.jstor.org/stable/20036706.

Young, I. R., E. Sanina, and A. V. Babanin. 2017. "Calibration and Cross Validation of a Global Wind and Wave Database of Altimeter, Radiometer, and Scatterometer Measurements." *Journal of Atmospheric and Oceanic Technology* 34, no. 6 (April): 1285–1306. ISSN: 0739-0572, accessed March 1, 2020. doi:10.1175/JTECH-D-16-0145.1. https://journals-ametsoc-org.eres.library.manoa.hawaii.edu/doi/full/10.1175/JTECH-D-16-0145.1.

Young, I. R., S. Zieger, and A. V. Babanin. 2011. "Global Trends in Wind Speed and Wave Height" [in en]. *Science* 332, no. 6028 (April): 451–455. ISSN: 0036-8075, 1095-9203, accessed September 2, 2019. doi:10.1126/science.1197219. http://www.sciencemag.org/cgi/doi/10.1126/science.1197219.

Young, Ian R., and Agustinus Ribal. 2019. "Multiplatform evaluation of global trends in wind speed and wave height" [in en]. *Science* 364, no. 6440 (May): 548–552. ISSN: 0036-8075, 1095-9203, accessed March 1, 2020. doi:10.1126/science.aav9527. https://science-sciencemag-org.eres.library.manoa.hawaii.edu/content/364/6440/548.

Zieger, S., J. Vinoth, and I. R. Young. 2009. "Joint Calibration of Multiplatform Altimeter Measurements of Wind Speed and Wave Height over the Past 20 Years" [in en]. Publisher: American Meteorological Society, *Journal of Atmospheric and Oceanic Technology* 26, no. 12 (December): 2549–2564. ISSN: 0739-0572, accessed July 20, 2020. doi:10.1175/2009JTECHA1303.1. https://journals-ametsoc-org.eres.library.manoa.hawaii.edu/jtech/article/26/12/2549/3240/Joint-Calibration-of-Multiplatform-Altimeter.